Supplementary Information for the manuscript

A Neandertal dietary conundrum: new insights provided by Zn isotopes at Gabasa, Spain

Klervia Jaouen, Vanessa Villalba-Mouco, Manuel Trost, Geoff M. Smith, Jennifer Leichliter, Tina Lüdecke, Pauline Méjean, Stéphanie Mandrou, Jérôme Chmeleff, Danaé Guiserix, Nicolas Bourgon, Fernanda Blasco, Jéssica Mendes Cardoso, Camille Duquenoy, Zineb Moubtahij, Domingo C. Salazar Garcia, Michael Richards, Thomas Tütken, Jean-Jacques Hublin, Pilar Utrilla, Lourdes Montes

Supplementary Information 1

Environmental, geological and zooarcheological context of Gabasa 1

1. Stratigraphy and geology

The site of Gabasa (Los Moros cave) is located in the northeast of the Iberian Peninsula on a limestone escarpment in the sub-Pyrenees, approximately 780 m asl. The region of Gabasa is characterized by a sedimentary bedrock with Mesozoic and Cenozoic deposits (Figure S1). The sediments are siliciclastic rocks and limestones. Siliciclastic rocks are typically associated with δ^{66}Zn values around 0.28±0.13 ‰ (1). Limestones have values ranging from 0.4 to 1.4 ‰ (2). Based on other works in the Spanish Pyrenean mountains and the Ebro valley, the local Sr isotope ratios range from 0.7038 to 0.7189 (3–9). For the 146 data points we collected for the sediments in Gabasa's region, the average $^{87}Sr/^{86}Sr$ is 0.7086 ± 0.0038 2SD. The sandstones tend to exhibit the highest ratios. The Sr content ranges from 111 ppm (µg/g, samples rich in dolomite) to 1200 ppm (samples rich in calcite). The Zn content of the rocks in the Gabasa area ranges from 62 ppm (samples rich in calcite) to 120 ppm (10) (samples rich in illite).

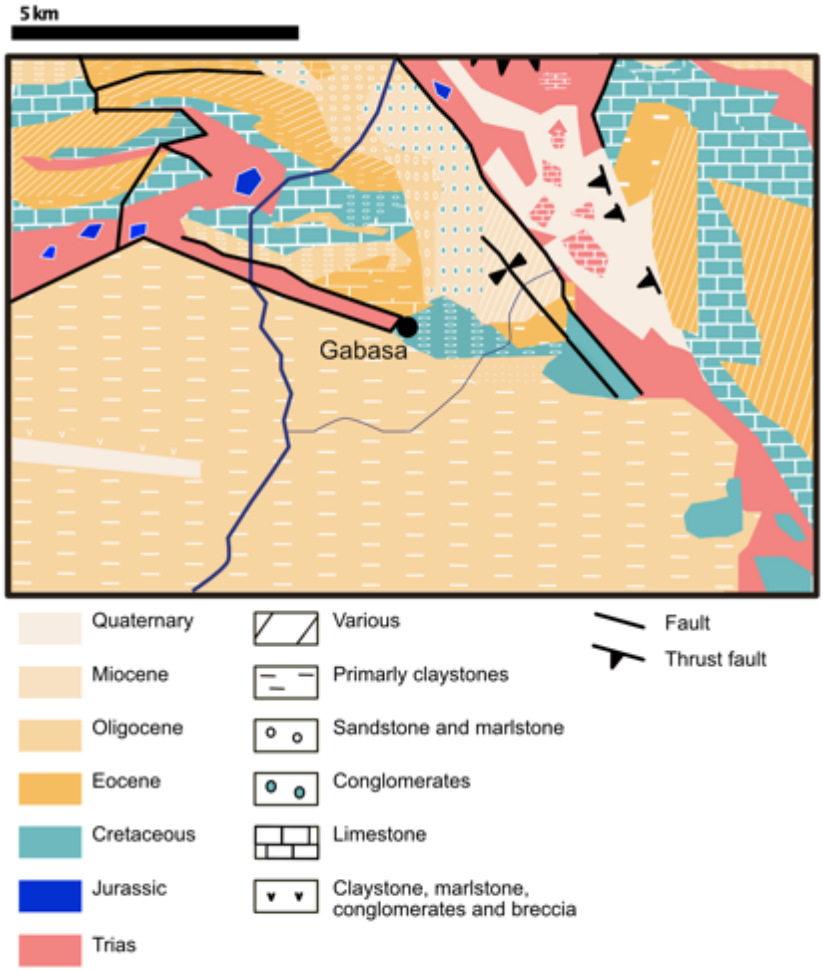

Figure S1: Simplified geological map of the Gabasa region based on the geological maps of Huesca and Lerida(11)**.**

The site is a cave in a Cretaceous limestone cliff partitioned into two distinct chambers with the Paleolithic occupation concentrated only in the second chamber, where excavations were conducted between 1984 and 1994 (12).

The archeological levels e, f, and g are characterized by a matrix of clays with carbonate components (blocks in layer e, and much smaller stone size fractions in layers f and g (Figure S2 (13)). The lithic material (stone tools and byproducts) of these three layers and the stratigraphy in general has been assigned to the Typical Mousterian "rich in scrapers", except for the upper ones (a and c) that could be associated to the Acheulean Tradition, Type B (14). Sedimentology shows a continuity between layers h, g and f, a clear hiatus between levels f and e, and a continuity over the rest of the stratigraphy. Therefore, layers g and f are probably dating back from Middle Pleistocene (which corresponds to the established age of the layer h), while for level e and later two options are considered: they could also be slightly younger but from the Middle Pleistocene, or MIS 3, if the AMS dating obtained in the 80's of level e is considered reliable (14).

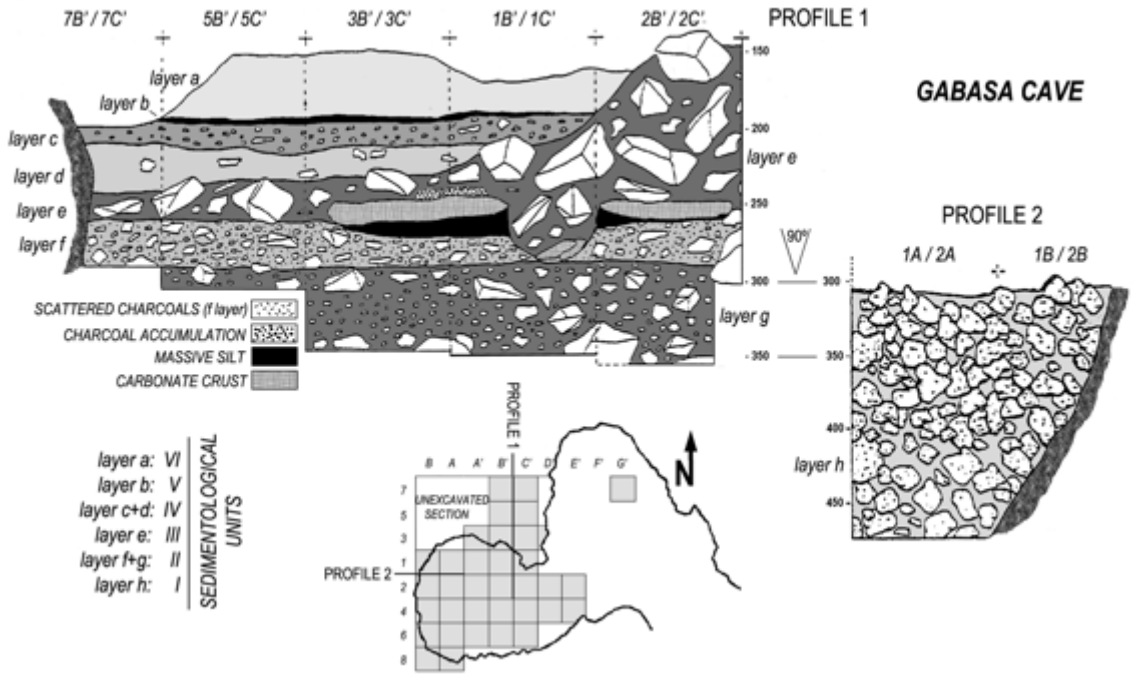

Figure S2: Reproduction of the stratigraphy from Gabasa already published in Montes and Pillar (2014)(12)**.**

2. Zooarcheological data

2.1 Species found in the layers e and f

According to the work of Blasco (14, 15), the main species – with the exclusion of the microfauna – found at Gabasa 1 in the levels e and f are: 1) European rabbit (*Oryctolagus cuniculus*) 2) Iberian ibex (*Capra pyrenaica*) 3) red deer (*Cervus elaphus*) and 4) wild horse (*Equus ferus*). Among the carnivores, the main species are 1) gray wolf (*Canis lupus*) and 2) cave hyena (*Crocuta spelaea*) (14) (Figure S3). The taxonomic identification of the teeth sampled was not always possible to species level. However, from the work of Blasco (14, 15), we know that the only bear (Ursus), hyena (Crocuta) and fox (Vulpes) species present at Gabasa were the cave bear [*Ursus spelaeus*], the cave hyena [*Crocuta spelaea*], and the red fox [*Vulpes vulpes*] (Figure S3).

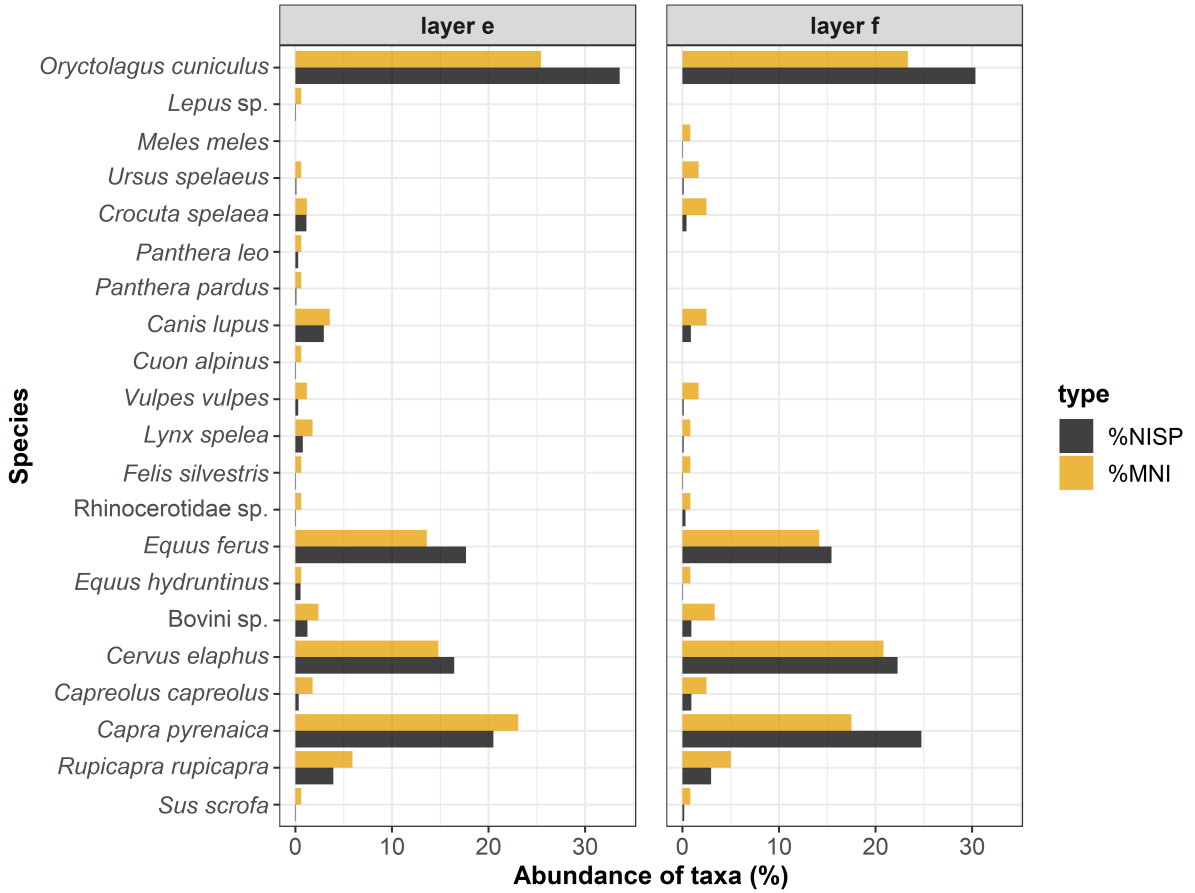

Figure S3: Percentage of minimum number of individuals (%MNI) and number of identifiable species (%NISP) from levels e and f at Gabasa.

2.2 Cut marks

In the layers e and f, cut marks were mostly identified on red deer and horses. The Iberian ibex and chamois do not have cut marks (Figure S4) and were likely accumulated by the other carnivores, mainly

wolves and hyenas (15). Some bone fractures indicate the consumption of bone marrow. Only 0.1 % of rabbit remains show cut marks (14), but the disarticulation of rabbits does not require the use of stone tools. Therefore, the low amount of anthropic modifications does not necessarily indicate the absence of the consumption of these animals (15). Nevertheless, the relatively high proportion of carnivore modifications recorded across these rabbit remains (5.1 %) also illustrates the importance of such species in the diet of other carnivores at the site, including fox and lynx (Figure S4).

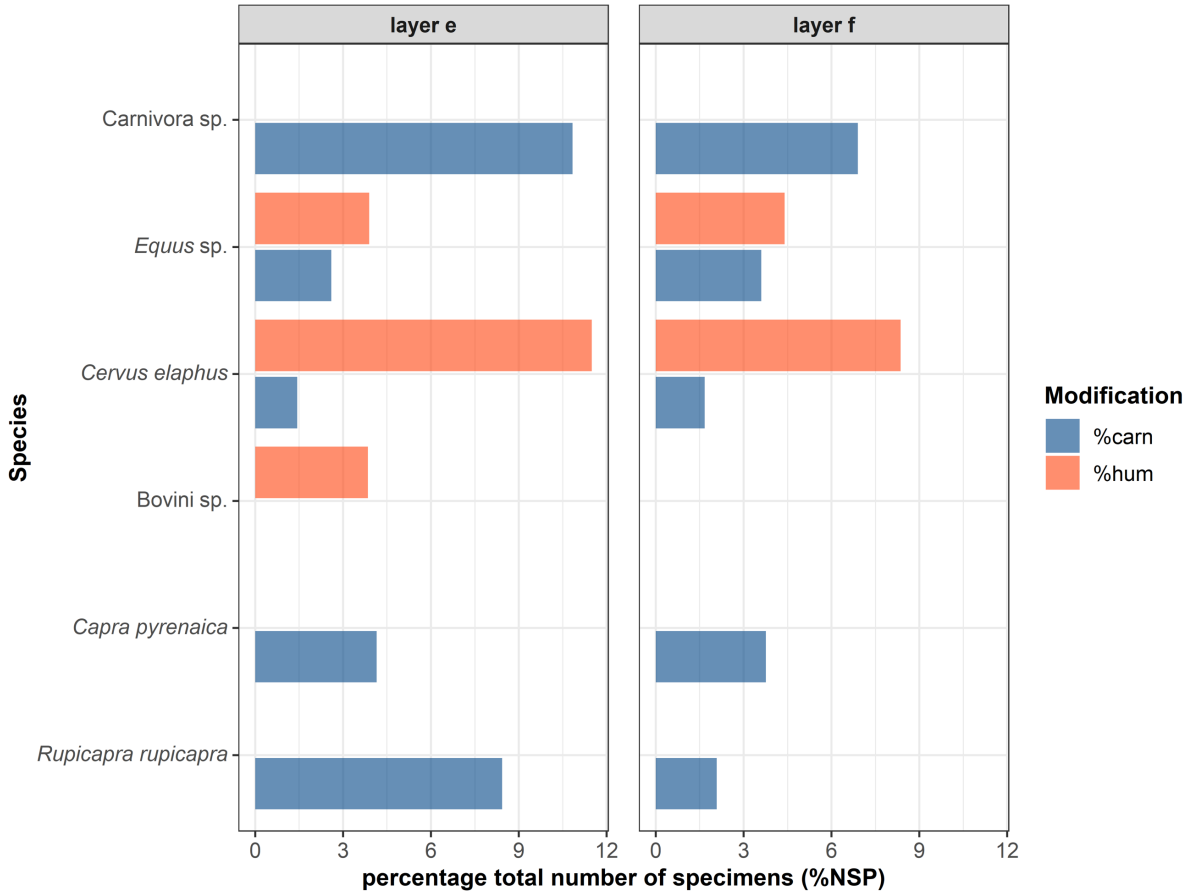

Figure S4: Percentages of specimens per species from Levels e and f showing carnivore (%carn) and/or human (%hum) modifications. Carnivore modifications include all types of modifications (tooth pits, scalloping, tooth scratches); Anthropogenic modifications include cut marks and marrow fractured bones. A detailed breakdown of modifications on rabbit bones is not provided but is given as percentages of all layers for carnivores (5.1 %) and humans (0.1 %). Data modified from Blasco (1997)(14).

2.3 Mortality of herbivore species

Remains of the mountain taxa Iberian ibex and chamois found at Gabasa are mostly from adult individuals (72 % and 62 %, respectively) and appear to have been the prey of carnivores. In contrast, deer and horse specimens include mostly juveniles (59 % and 61 %, respectively) and show a higher

occurrence of human modifications (14, 16). For those two species, about 40 % did not survive the first summer of their life (14, 15).

3. Paleoenvironments

Species can be grouped by biotope usage: horses thrived in open environments, chamois and ibex in the mountains, and deer in the forest. While the proportion of the minimum number of individuals for each group found in layers e, f and g varies and could indicate environmental changes, Gabasa predominantly consisted of a mosaic landscape where forest and open areas are present, but where open environments dominate during cold and arid stages. This corresponds to a typical environment of the Mediterranean mid-mountains.

Level g has the highest number of individuals from mountain habitats (23.4 % open environment; 25.3 % forest; 48.0 % mountain). Level f has a similar number of animals coming from open environments (26.5 %) but more deer than level g (36.5 % for the forest group). Level e comprised 40.1 % mountain species, 29.7 % forest dwellers, and 27.8 % taxa adapted to an open environment (Table S1).

Level	Open environment	Forest	Mountain
e	27.8%	29.7%	40.1%
f	26.5%	36.5%	27 %
g	23.4 %	25.3%	48.0%

Table S1. Proportion of species from three types of environments (open, forest and mountain) at Gabasa. Data are from Blasco (1995)(15)**.**

The paleoenvironmental interpretation of Gabasa has been debated over the last 30 years since reconstructions based on faunal, sedimentological, and pollen data often indicate different biomes in the stratigraphy of Gabasa, including layers e and f (Table S2) (12, 17). The sedimentological evidence (13), illustrates that the climate during the formation of the layers f and g was humid and cool to temperate, and becoming cooler in level e. Conversely, the faunal record suggests similar conditions for all three levels: temperate and humid (15) though the species may have had different environmental tolerances compared to modern day populations and distributions. Further, pollen analysis from hyena coprolites indicates a cool but dry climate for all three layers (18). Initially, all these paleoenvironmental data were framed in MIS 3 (specifically in Wurm II) according to the ^{14}C dates performed on charcoal – though such measurements are considered unreliable because of the very small amount of material analyzed in 1985 (16) (Table S2). After having obtained an amino acid racemization (AAR) date of *ca.* 140 ± 80 ka (16) for Unit I, it has been proposed that Unit II (layers f and g) may also correspond to the Middle Pleistocene as there are no erosion traces nor stratigraphic discontinuity between both units (12, 16). A clear discontinuity between layers e and f indicates a new sedimentary phase, which suggests that level e is of a younger age that has not been successfully determined to this day.

Layer	Sedimentology (Hoyos et al. 1992)	Pollen (González-Sampériz et al. 2004)	Zooarcheology (Blasco et al. 1995)	Chronology (Utrilla et al. 2010)
e	Cool and humid	Cool and dry	Temperate and humid	46,500 + 4,400 -2,800 or >51,900?
f	Temperate to cool and humid	Cool and dry	Temperate and humid	MIS 5?
g	Temperate to cool and humid	Cool and dry	Temperate and humid	MIS6? > 50,700 ?

Table S2: Climate interpretation according to zooarcheology, pollen or sedimentology for the layers e, f and g. Contradictions can be seen depending on the method used (12–16, 18).

Supplementary Information 2

Supplementary Information on the material and methods

2.1 Strategy during the material selection

2.1.1 Species selection

To evaluate the diet of the studied Neandertal specimen of Gabasa, we included fauna that possibly had a similar diet to Neandertals and/or that were likely consumed by them. We therefore selected:

- The most abundant species (European rabbit, red deer, Iberian ibex, chamois, wild horses)
- The maximum diversity of carnivorous species to ensure distinguishing different types of carnivorous diets (Table S3).

Species	**Diet**	**Reference**
Cave lynx *(Lynx spelaea)*	Lagomorphs (such as *O. cuniculus*), rodents, birds	(19)
Red fox *(Vulpes vulpes)*	Lagomorphs (such as *O. cuniculus*), other small mammals, birds, ungulates, insects	(20)
Cave hyena *(Crocuta spelaea)*	Red deer (*C. elaphus*), chamois (*R. rupicapra*), ibex (*C. pyrenaica*)	(21, 22)
Gray wolf *(Canis lupus)*	Wild ungulates	(23–25)
Dhole *(Cuon alpinus)*	Ungulates (possibly preferentially *R. rupicapra*), birds, rodents	(26, 27)

Table S3: Primary food source of carnivorous species from Gabasa 1 according to modern or zooarcheological data.

2.1.2 Sampling strategy

The dental enamel of archeological specimens from Gabasa generally showed good preservation, but some teeth presented a high number of cracks filled with manganese oxides (Figure S5). In cracked teeth, we did not sample the full height of the crowns to minimize accidental fracture of the teeth and avoid contamination from sediment found in those cracks. To evaluate potential seasonal and migration patterns (using Zn and Sr isotope ratios), several different samples were taken from the enamel of each

tooth whenever possible (Table S4), and sequential sampling was performed for one horse tooth (SEVA 34414). Dentin was also sampled for four teeth (34408, 34409, 35054, and 35057) and cementum for one (35057) to conduct Zn isotope analyses to identify potential diagenesis effect (Table S4).

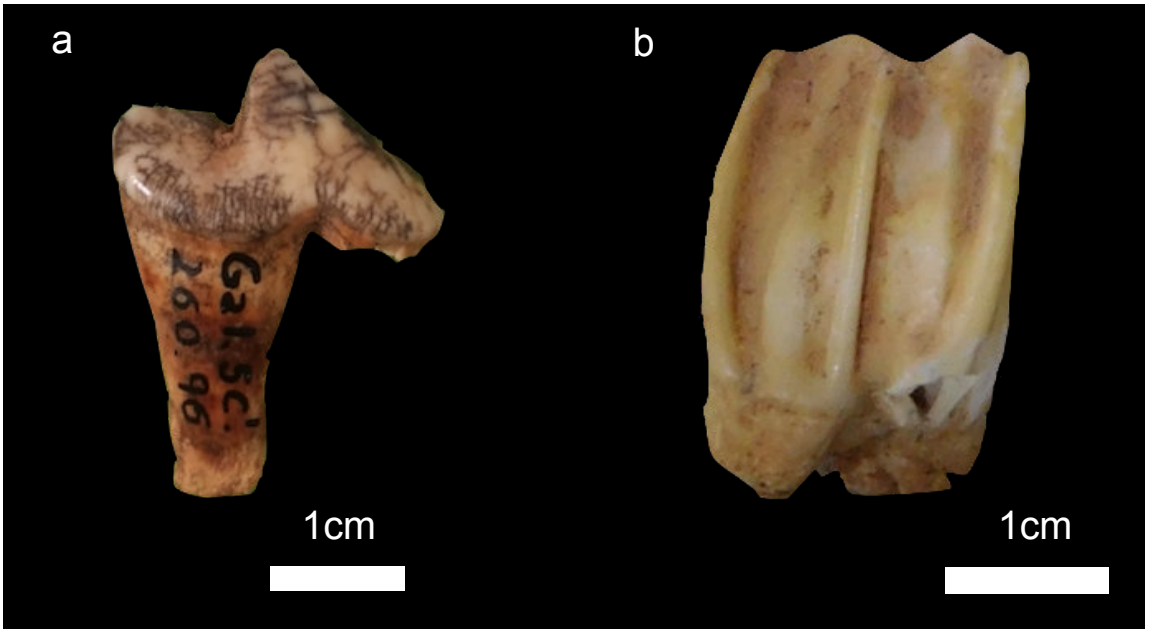

Figure S5: a) P4 of a dhole *Cuon alpinus* (level e) and b) molar of a chamois *Rupicapra rupicapra* (level f). The two teeth show very different state of preservation. Cracks with manganese oxides were not sampled.

										Number of samples taken per proxy analyzed			
Id SEVA	Id ARCH	Id museum	Species	Common name	Layer	Tissue sampled	Tooth sampled	Diet	Environment	Zn isotopes	C and O isotopes	Sr isotopes	Trace elements
34408	78	Ga1.2B.255.265	*Canis lupus*	Grey wolf	e	dental enamel	P4	Carnivore	NA	3	1	1	1
34409	79	Ga1.1C.217.13	*Canis lupus*	Grey wolf	e	dental enamel	M1?	Carnivore	NA	2	1	1	1
34410a		Ga1.5C.327.169	*Ursus* sp.	Bear	f	dental enamel	M2	Omnivore	Cave	1	1	0	1
34410b		Ga1.5C.348.546	*Ursus* sp.	Bear	f	dental enamel	M2	Omnivore	Cave	2	0	0	1
34411		Ga1.8B.205.103.(26)	*Crocuta* sp.	Hyena	e	dental enamel	M1?	Bone eating carnivore	Cave	2	1	0	1
34412		Ga1.5C.260.96	*Cuon* sp.	Dhole	e	dental enamel	P4?	Carnivore	NA	1	1	0	1
34413		Ga1.3A'.263.49	*Rupicapra rupicapra*	Chamois	f	dental enamel	P3	Herbivore	Mountain	2	1	1	1
34414	82 to 85, 95	Ga1.4A'.239.75(96)	*Equus ferus*	Horse	e	dental enamel	P	Herbivore	Open	7	4	5	1
34415		GA15c'244 17	*Equus ferus*	Horse	e	dental enamel	P	Herbivore	Open	2	1	0	1
34416		GA 1 3C' 285 73	*Equus ferus*	Horse	f	dental enamel	P or M	Herbivore	Open	2	1	0	1
34417	86	GA13A'285 89	*Cervus elaphus*	Red deer	f	dental enamel	M	Herbivore	Forest	1	1	1	1
34418	87	Ga1.4C'.177-116	*Equus hydrontinus*	European wild ass	e	dental enamel	P or M	Herbivore	Open	2	1	1	1
34419		GA1 4a 240 3 (19)	*Equus ferus*	Horse	f	dental enamel	P or M	Herbivore	Open	2	1	0	1
34420		Ga1.3C'.240	*Canis lupus*	Wolf	e	dental enamel	P4 ?	Carnivore	NA	2	1	0	1
34421		Ga1.8B.210.70(51)	*Vulpes* sp.	Fox	e	dental enamel	P3	Carnivore	NA	2	1	0	1
34422	80	Ga1 rev 303	*Homo neanderthalensis*	Neandertal	rev	dental enamel	M1	NA	NA	1	1	1	1
35034	88	rabbit e	*Oryctolagus cuniculus*	European rabbit	e	dental enamel	?	Herbivore	NA	1	1	1	1
35035	89	rabbit e	*Oryctolagus cuniculus*	European rabbit	e	dental enamel	?	Herbivore	NA	1	0	1	1
35036	90	rabbit e	*Oryctolagus cuniculus*	European rabbit	e	dental enamel	?	Herbivore	NA	1	1	1	1
35037	91	rabbit e	*Oryctolagus cuniculus*	European rabbit	e	dental enamel	?	Herbivore	NA	1	1	1	1
35038	92	rabbit e	*Oryctolagus cuniculus*	European rabbit	e	dental enamel	?	Herbivore	NA	1	1	1	1
35045	96	Ga1.6A.209.72	Cervid	Deer	e	dental enamel	M1	Herbivore	Forest	1	1	1	1
35046		GA1-BA-230-220	*Canis* sp.	Wolf	e	dental enamel	P or M	Carnivore	NA	1	0	0	0
35047		GA1-BA-230-1B12	*Canis* sp.	Wolf	e	dental enamel	P or M	Carnivore	NA	1	0	0	0
35048		GA1-BA-225-310	*Canis* sp.	Wolf	e	dental enamel	P or M	Carnivore	NA	1	0	0	0
35049		Rabbit tooth E1	*Oryctolagus cuniculus*	European rabbit	e	dental enamel	?	Herbivore	NA	1	1	0	1
35050		Rabbit tooth E2	*Oryctolagus cuniculus*	European rabbit	e	dental enamel	?	Herbivore	NA	1	1	0	1
35051		Rabbit tooth E3	*Oryctolagus cuniculus*	European rabbit	e	dental enamel	?	Herbivore	NA	1	1	0	1
35052		Ga1.5C.352.577	*Ursus* sp.	Bear	f	dental enamel	M2	Omnivore	Cave	1	1	0	1
35053	97	Lib'289-198	*Capra pyreneica*	Ibex	f	dental enamel	M2	Herbivore	Mountain	1	1	1	1
35054		GA16B 245 119	*Capra pyreneica*	Ibex	f	dental enamel	M2	Herbivore	Mountain	2	1	0	1
35055		GA18B219 795-511	*Vulpes* sp.	Fox	e	dental enamel	P2	Carnivore	NA	1	0	0	0
35056		whole tooth lvl g	*Vulpes* sp.	Fox	g	dental enamel	dp4	Carnivore	NA	1	1	0	1
35057	93	Ga1.1C'.336.422	*Equus hydrontinus*	European wild ass	e	dental enamel	P or M	Herbivore	Open	1	1	1	1
35058		lynx	*Lynx spelaea*	Cave lynx	f	dental enamel	P4	Carnivore	NA	3	1	0	1
35059	94	GA1B 26 024 436	*Crocuta* sp.	Hyena	f	dental enamel	P3	Bone eating carnivore	Cave	1	1	1	1
35060		Ga1.6E.260.191	*Crocuta* sp.	Hyena	f	dental enamel	C	Bone eating carnivore	Cave	1	1	0	1
35061	98	Ga1.5B.282.42	*Crocuta* sp.	Hyena	f	dental enamel	C	Bone eating carnivore	Cave	1	1	1	1
35062		GA16G2322960a	*Rupicapra rupicapra*	Chamois	f	dental enamel	M3	Herbivore	Mountain	1	1	0	1
35063		GA16G2322960b	*Rupicapra rupicapra*	Chamois	f	dental enamel	M3	Herbivore	Mountain	1	1	0	1
35064		Ga1.2B.235.125.67	*Cervus elaphus*	Red deer	e	dental enamel	M1	Herbivore	Forest	1	1	0	1
35065		Ga1.3B.290.82	*Cervus elaphus.*	Red deer	e	dental enamel	M2	Herbivore	Forest	1	1	0	0
35066		GA1K224-66	*Canis* sp.	Wolf	e	dental enamel	P4	Carnivore	NA	1	1	0	1
35067	99	Ga1.7C.290.109	*Crocuta* sp.	Hyena	f	dental enamel	P3	Bone eating carnivore	Cave	1	1	1	1
35068		Ga1.6A.200.28	*Rupicapra rupicapra*	Chamois	e	dental enamel	M1/M2	Herbivore	Mountain	1	1	0	1

Table S4. General information related to the sample strategy of this study (species, identification numbers, layers, teeth and tissues sampled, proxy analyzed). Id museum: identification number of the Huesca Museum. Id SEVA: identification number at the MPI-EVA (Max Planck Institute for Evolutionary Anthropology). Id ARCH: identification number at the GET (Géosciences Environnement Toulouse)

2.2 Accuracy of trace elements as well as Zn, C, O, and Sr isotope measurements

We measured two external standards for Zn isotope analyses: SRM 1400 and AZE. Their values are statistically indistinguishable from values reported in other studies, indicating the robustness of our data (Table S5). All measured samples and standards showed mass-dependent isotope fractionation. Zinc isotope mass-independent fractionation for biological samples would have revealed instrumental bias or interferences due to an insufficient purification of the zinc. Procedural blanks contained only 1 to 5 ng of Zn.

This study

	δ^{66}Zn (‰- JMC Lyon)	1SD		δ^{66}Zn (‰- JMC Lyon)	1SD
AZE 9	1.42		SRM 1400 27	0.98	0.06
AZE 10	1.59		SRM 1400 45	0.90	0.03
AZE 11	1.50		SRM 1400 59	0.88	
AZE 18	1.65				
AZE 25	1.63				
AZE 32	1.58				
AZE (mean)	**1.56**	**0.09**	**SRM 1400 (mean)**	**0.92**	**0.05**

Expected values

	δ^{66}Zn (‰- JMC Lyon)	1SD		δ^{66}Zn (‰- JMC Lyon)	1SD
Jaouen (2012)	1.50	0.04	Jaouen et al. (2018)	1.00	0.04
Jaouen et al. (2016a)	1.51	0.12	Bourgon et al. (2020)	0.94	0.05
Jaouen et al. (2016b)	1.50	0.11	Jaouen et al. (2020)	1.00	0.07
Jaouen et al. (2018)	1.65	0.14	McCormack et al. (2021)	0.95	0.03
Bourgon et al. (2020)	1.63	0.05	Bourgon et al. (2021)	0.96	0.01
Jaouen et al. (2020)	1.58	0.06			
Bourgon et al. (2021)	1.60	0.00			
AZE (mean)	**1.57**	**0.06**	**SRM 1400 (mean)**	**0.97**	**0.03**

Table S5. Zinc isotope results for the SRM 1400 and AZE reference material and in house standard(28–35)**.** The number following the reference material's names correspond to the identification number of a specific preparation of this material.

Strontium isotope values were normalized using the reference material SRM 987 ($^{87}Sr/^{86}Sr$=0.70924) that was measured with samples in each measurement session. The offset between the measured and the true value was 0.00004 (Table S6). The reference materials measured for Sr were the standards SRM 1486 and SRM 1400, and their values fit with the long-term compiled value of the Max Planck Institute for Evolutionary Anthropology (Table S6).

This study

	$^{87}Sr/^{86}Sr_{uncorr}$	SE	$^{87}Sr/^{86}Sr_{corr}$	SE	Analyzed with
SRM 1486	0.709349	7.84.10-6	0.709309	$5.38.10^{-6}$	Triton Plus
SRM1486 405	0.709383	1.25.10-5	0.709343	$1.24.10^{-5}$	Triton Plus
SRM 1486 407	0.709349	1.14.10-5	0.709309	$1.14.10^{-5}$	Triton Plus
SRM 1486 393	0.709336	3.52.10-6	0.709296	$3.52.10^{-6}$	Triton Plus
SRM 1486 371	0.709333	5.49E-06	0.709279	$5.49.10^{-6}$	Neptune Plus

	$^{87}Sr/^{86}Sr_{corr}$	SD
Average	0.709307	2.34989E-05

Expected value

	$^{87}Sr/^{86}Sr_{corr}$	SD
Jaouen et al. 2018(35)	0.709299	0.000027

Table S6. Sr isotope results for the SRM 1486 standard

Four reference materials were run along samples during C and O isotope analyses (IAEA, VICS, NIST SRM120c, NBS 18) using the coldtrap method of Vonhof et al. (2020) (36). Quality control parameters are given in the Table S7.

	measured					**true value**		
Std	corrected $\delta^{13}C$ (‰) V-PDB	corrected $\delta^{18}O$ (‰) V-PDB	SD $\delta^{13}C$	SD $\delta^{18}O$	n	corrected $\delta^{13}C$ (‰) V-PDB	corrected $\delta^{18}O$ (‰) V-PDB	ref
VICS	1.25	-5.12	0.19	0.20	24	1.25	-5.44	Vonhof et al (2020)(36)
IAEA-603	2.14	-2.04	0.32	0.25	15	2.46	-2.37	nucleus.iaea.org
NBS 18	-4.94	-21.90	0.15	0.94	9	-5.01	-22.97	Stichler (1995)(37)
NIST SRM 120c	-6.32	-2.00	0.26	0.27	14	-6.3	-0.98 to -2.8	GeoReM(38)

Table S7. Reference materials used for stable C and O isotope analyses.

For the trace elements, the multi-element standard solution EPOND and the reference material SLRS6 (39) were measured twice along with the other Gabasa samples, using a triple quadrupole ICP-MS (iCapTQ, Thermoscientific) (Observatoire Midi Pyrénées OMP, Toulouse France). A calibration line was established to fit with the range of the concentration observed in bones and teeth, and the Ca concentration of the EPOND standard solution was out of the range (concentration too low) and was therefore not measured. Other elements gave concentration in the range of what is expected for these two reference materials (Table S8).

	Al	Ca	Mn	Cu	Zn	Sr	Ba
SLRS6	27.7	8689	2.05	25.8	2.0	40.45	16.40
Expected value	33.8	8760	2.12	23.9	1.76	40.66	14.28
SD	2.2	200	0.06	7.5	0.12	0.32	0.48
EPOND	863	out of calibration range	929	999	922	1004	1140
Expected value	1000	1000	1000	1000	1000	1000	1000
SD	5	5	5	5	5	5	5

Table S8. Trace element results for the standard solution EPOND and the reference material SLRS6 (in ppm)

2.3 Collagen extraction

Sample ID (S-EVA)	Taxon	sample mass (mg)	>30 kd (mg)	<30 kd	% of collagen	notes
34413	*R. rupicapra*	211.5	0.1	no collagen	_	no collagen
34421	*Vulpes* sp.	104.4	0.7	no collagen	0.671	
35056	*Vulpes* sp.	227.5	0.6	no collagen	_	no collagen
35058	*Lynx* sp.	219.2	0.4	no collagen	0.183	

Table S9. Results of the collagen extraction. S-EVA corresponds to the code for the samples analyzed for stable isotopes at the Department of Human Evolution of the Max Planck Institute for Evolutionary Anthropology. 30 kD corresponds to the mass of collagen that was ultrafiltered at more than 30 kD, and the <30 kD was the mass of collagen in the liquid that went through the filter (molecules smaller than 10 kD)

The extraction did not yield any or less than 1 % of collagen (Table S9), and therefore did not meet the criterion for radiocarbon dating. We were able to run C and N isotope analyses only for sample 34421 (*Vulpes* sp.; Table S10). However, its C:N ratio was above 3.6, which indicates that the collagen was altered. Therefore, this sample cannot be included in the discussion as stable isotope results do not give reliable dietary information due to this bad preservation, even if its nitrogen isotope ratio is in the expected range for foxes.

Sample ID (S-EVA)	Taxon	δ^{13}C corr (‰)	δ^{15}N corr (‰)	%C	%N	C/N
34421 a	*Vulpes* sp.	-21.00	11.35	46.79	12.36	4.4
34421 b	*Vulpes* sp.	-20.55	11.19	46.24	13.06	4.1

Table S10. C and N isotope results for sample 34421.

Supplementary Information 3

Supplementary information on diagenesis

The interpretation of the diet and mobility of the Neandertal and contemporaneous mammals at Gabasa depends on the preservation of biogenic signatures in the material analyzed. We chose to work on dental enamel, which is more resistant to diagenesis than bones due to its dense, highly mineralized, and chemically resistant bioapatite mineral matrix (40, 41). We analyzed various tracers of mobility and diet (C, O, Zn, and Sr isotopes, and Ba/Ca and Sr/Ca trace element ratios), all of which are not necessarily impacted by diagenetic events to the same extent. In order to investigate if the C, O, Zn, Sr, and Ba content in Gabasa mammal teeth could be of taphonomical origin, we decided to

1) Assess the presence or absence of correlation between element contents and their isotope composition, which could represent a mixing line between a biogenic and a diagenetic pole (42). This can be achieved through a simple regression $\delta^{YY}X=a(1/[X])+b$, whereby "$\delta^{YY}X$" is one of the delta values of the element "X" (e.g., $\delta^{66}Zn$, $\delta^{67}Zn$ or $\delta^{68}Zn$ for zinc), "[X]" is its content, "a" is the slope and "b" is the intersection with the y axis.
2) Compare the content of elements with values reported in modern enamel for the elements of interest (C, O, Zn, Sr, and Ba) and for elements known to be much more concentrated in soils than in teeth, and therefore likely to trace the integration of diagenetic components (Al, Mn, Fe).
3) Explore if a correlation exists between elements of interest or their isotope composition and the concentration of elements likely to be of diagenetic origin (Al, Mn, Fe) (Table S12).
4) Explore if the abovementioned correlations still exist when the samples presenting abnormal trace element contents are excluded. (Table S13).
5) Explore if specimens without visible alterations had different trace element contents or isotope ratios compared to samples stained or cracked (Table S14).
6) Collect a few dentin samples (prone to diagenetic alteration) to compare their element content to dental enamel.

3.1 Correlation between isotope ratios and elemental content

- Zn isotope values and concentrations are not correlated (Multiple R-squared: 0.1062, Adjusted R-squared: 0.08545, F-statistic: 5.111 on 1 and 43 DF, p-value: 0.02889) which argues for the absence of diagenesis.
- We tested the correlation between $1/[CO_3]$ and $\delta^{13}C$ values, which shows an R^2 of 0.1.

- We tested the correlation between Ca/Sr and $^{87}Sr/^{86}Sr$, which shows an R^2 of 0.14. However, trace element concentrations and isotope measurements for each specimen were derived from two different samples of the same tooth (see 3.2).

3.2 Elemental compositions and ratios for tracing diagenetic effects

As insufficient sample powder was left for trace element studies, the same teeth were sampled another time. The powder samples were obtained by drilling close to the first sample point to get chronologically-compatible information with the isotope (C, O, Zn, Sr) analyses. However, there was insufficient material for trace element analyses for five of the 45 teeth sampled for this study. One tooth was sampled five times (34414). After visual inspection, 37 of the 42 trace element samples were described as "normal", seven as "stained". This visual classification was made to test if a correlation between the trace element content and the preservation of the sample is apparent which happened to be the case. However, we clearly acknowledge the limitations of this purely visible classification.
All trace elements' results and the color of the samples are given Table S11.

Id SEVA	Species	Sample type	Ba/Ca	Sr/Ca	Ba/Sr	Mn/Ca	Al/Ca	Cu/Ca	Zn/Ca	Fe/Ca	Excluded	Comment
34408d	*Canis lupus*	dentine	4.22E-04	1.13E-03	3.73E-01	6.68E-05	7.35E-05	5.18E-05	6.94E-04	5.17E-05	yes	stained
34408e	*Canis lupus*	enamel	2.06E-04	9.82E-04	2.10E-01	7.31E-05	3.64E-05	3.05E-05	3.35E-04	4.07E-05	no	normal
34409d	*Canis lupus*	dentine	3.30E-04	1.15E-03	2.86E-01	3.65E-04	9.83E-05	**8.91E-05**	5.88E-04	8.51E-05	yes	stained
34409e	*Canis lupus*	enamel	1.13E-04	5.54E-04	2.04E-01	1.04E-04	4.79E-05	2.73E-05	2.34E-04	7.01E-05	no	normal
34410a	*Ursus* sp.	enamel	1.31E-04	8.43E-04	1.56E-01	4.37E-05	2.66E-05	1.19E-05	1.74E-04	2.52E-05	no	normal
34410b	*Ursus* sp.	enamel	1.06E-04	8.46E-04	1.25E-01	1.17E-05	2.22E-05	6.32E-06	1.30E-04	1.65E-05	no	normal
34411	*Crocuta* sp.	enamel	5.86E-05	1.39E-03	4.23E-02	6.01E-05	1.25E-05	5.45E-06	2.64E-04	2.38E-05	no	stained
34412	*Cuon* sp.	enamel	8.76E-05	8.52E-04	1.03E-01	**1.03E-03**	3.50E-05	6.38E-06	1.66E-04	5.71E-05	yes	stained
34413	*Rupicapra rupicapra*	enamel	1.67E-04	4.22E-04	3.95E-01	1.26E-05	1.81E-05	1.13E-05	1.92E-04	1.41E-05	no	normal
34414	*Equus ferus*	enamel	9.20E-05	8.56E-04	1.08E-01	4.72E-05	2.46E-05	3.31E-06	1.02E-04	3.51E-05	no	normal
34415	*Equus ferus*	enamel	1.64E-04	1.21E-03	1.36E-01	2.98E-05	2.21E-06	1.11E-05	1.33E-04	1.33E-05	no	normal
34416	*Equus ferus*	enamel	9.77E-05	5.79E-04	1.69E-01	8.22E-05	1.17E-05	4.38E-06	9.77E-05	1.79E-05	no	stained
34417	*Cervus* sp.	enamel	4.60E-05	4.46E-04	1.03E-01	2.04E-05	7.39E-06	1.41E-05	1.33E-04	2.14E-05	no	normal
34418	*Equus hydrontinus*	enamel	7.67E-05	6.40E-04	1.20E-01	3.47E-05	5.73E-06	2.34E-06	**8.08E-05**	1.52E-05	no	normal
34419	*Equus ferus*	enamel	8.84E-05	9.52E-04	9.28E-02	**6.06E-06**	9.73E-06	2.48E-06	9.47E-05	1.95E-05	no	normal
34420	*Canis lupus*	enamel	2.01E-04	1.49E-03	1.35E-01	3.95E-05	5.38E-05	3.02E-05	2.77E-04	3.43E-05	no	normal
34421	*Vulpes* sp.	enamel	2.99E-04	4.90E-04	6.11E-01	2.61E-04	6.05E-05	2.14E-05	2.53E-04	4.06E-05	no	stained
34422e	*Homo neanderthalensis*	enamel	**1.78E-05**	5.16E-04	**3.44E-02**	4.79E-05	4.62E-05	1.66E-05	4.69E-04	5.42E-05	no	normal
35034	*Oryctolagys cuniculus*	enamel	4.96E-04	6.37E-04	7.79E-01	3.09E-04	3.91E-05	4.22E-05	4.18E-04	1.12E-03	yes	stained
35035	*Oryctolagys cuniculus*	enamel	3.15E-04	7.37E-04	4.27E-01	1.89E-04	3.99E-05	3.44E-05	3.39E-04	**2.31E-03**	yes	normal
35036	*Oryctolagys cuniculus*	enamel	2.85E-04	4.23E-04	6.73E-01	2.67E-05	1.23E-05	1.12E-05	2.63E-04	1.92E-05	no	normal
35037	*Oryctolagys cuniculus*	enamel	3.76E-04	1.11E-03	3.40E-01	2.40E-04	1.28E-04	3.96E-05	3.86E-04	1.41E-04	yes	stained
35038	*Oryctolagys cuniculus*	enamel	**5.62E-04**	9.14E-04	6.15E-01	5.73E-04	**2.81E-04**	**8.86E-05**	**7.96E-04**	2.64E-04	yes	stained
35045	*Cervid*	enamel	4.87E-04	6.03E-04	8.08E-01	4.94E-05	6.57E-05	2.02E-05	2.61E-04	6.48E-05	no	normal
35049	*Oryctolagys cuniculus*	enamel	2.88E-04	4.22E-04	6.84E-01	4.75E-05	1.18E-05	8.64E-06	2.28E-04	2.21E-05	no	normal
35050	*Oryctolagys cuniculus*	enamel	2.36E-04	7.66E-04	3.08E-01	1.19E-04	5.49E-05	1.90E-05	3.64E-04	2.42E-05	no	normal
35051	*Oryctolagys cuniculus*	enamel	1.98E-04	5.63E-04	3.52E-01	3.46E-05	1.16E-05	5.34E-06	2.28E-04	1.87E-05	no	normal
35052	*Ursus* sp.	enamel	8.08E-05	3.54E-04	2.28E-01	8.88E-06	1.66E-05	**1.22E-06**	1.04E-04	**8.06E-06**	no	normal
35053	*Capra pyreneica*	enamel	2.53E-04	6.14E-04	4.12E-01	1.52E-05	9.78E-06	6.68E-06	9.04E-05	1.61E-05	no	normal
35054	*Capra pyreneica*	enamel	2.10E-04	**2.41E-04**	8.72E-01	6.85E-06	6.25E-06	2.84E-06	1.29E-04	1.23E-05	no	normal
35056	*Vulpes* sp.	enamel	5.80E-05	3.52E-04	1.65E-01	4.05E-05	2.54E-05	5.09E-06	1.85E-04	1.78E-05	no	normal
35057	*Equus hydrontinus*	enamel	8.23E-05	7.98E-04	1.03E-01	8.11E-06	1.05E-05	2.22E-06	1.08E-04	1.24E-05	no	normal
35058	*Lynx speleae*	enamel	6.84E-05	5.67E-04	1.21E-01	2.06E-04	6.00E-06	2.19E-06	1.50E-04	1.74E-05	no	normal
35059	*Crocuta* sp.	enamel	8.05E-05	1.52E-03	5.29E-02	1.44E-05	8.80E-06	2.49E-06	1.70E-04	9.05E-06	no	normal
35060	*Crocuta* sp.	enamel	8.31E-05	8.03E-04	1.03E-01	5.20E-05	8.70E-06	4.33E-06	2.18E-04	1.14E-05	no	normal
35061	*Crocuta* sp.	enamel	6.35E-05	5.30E-04	1.20E-01	3.64E-05	2.06E-06	2.26E-06	1.30E-04	1.56E-05	no	normal
35062	*Rupicapra rupicapra*	enamel	2.20E-04	2.44E-04	**9.02E-01**	1.08E-05	5.88E-06	2.21E-06	1.99E-04	1.47E-05	no	normal
35063	*Rupicapra rupicapra*	enamel	2.41E-04	2.84E-04	8.48E-01	3.00E-05	1.11E-05	9.98E-06	2.50E-04	1.90E-05	no	normal
35064	*Cervus* sp.	enamel	1.65E-04	2.94E-04	5.62E-01	8.45E-06	**1.01E-06**	1.56E-06	1.71E-04	1.10E-05	no	normal
35066	*Canis* sp.	enamel	6.17E-05	6.77E-04	9.12E-02	3.13E-05	1.85E-05	1.04E-05	1.88E-04	3.23E-05	no	normal
35067	*Crocuta* sp.	enamel	5.88E-05	**1.70E-03**	3.45E-02	1.12E-04	1.74E-05	1.03E-05	2.96E-04	1.45E-05	no	normal
35068	*Rupicapra rupicapra*	enamel	2.59E-04	3.62E-04	7.15E-01	1.83E-04	2.39E-05	2.92E-06	9.74E-05	1.66E-05	no	normal

Table S11. Ratios of trace element to Ca in teeth of Gabasa mammals. Id SEVA corresponds to the identification number at the MPI-EVA (Max Planck Institute for Evolutionary Anthropology). The column "Excluded" corresponds to the samples excluded from biogenic interpretation because the content of one or several trace elements is too high to be considered non-diagenetic. The column "comment" corresponds to the visual appearance of the enamel sample. Blue numbers correspond to minimal values, red ones to maxima.

In order to assess potential soil contamination, we chose to analyze Al, Mn, Fe that show elevated concentrations in various soils but not in teeth (43). As the amount of tooth (enamel and dentin) sampled

was really low, we express the Al, Mn, Fe content as Al/Ca, Mn/Ca, Fe/Ca ratios to avoid misevaluation of the actual content due to error on the sample mass. The two dentin samples (Table S11) had a trace element content slightly higher than the associated enamel samples but with the same order of magnitude. The Al/Ca, Mn/Ca, and Fe/Ca ratios in dental enamel were mostly comprised, respectively, between 1 10^{-6} to 7 10^{-6}, 8 10^{-6} to 7 10^{-4}, and 6 10^{-6} to 2 10^{-3}. A few exceptions exist:

- Samples 35037 and 35038, two rabbit teeth, showed higher enamel Al/Ca ratios than all other enamel samples (1.4 10^{-4} and 3.2 10^{-4}, respectively). The samples were noted to be "stained" (Table S11).
- Samples 34412 and 35038, one dhole tooth and one of the two abovementioned rabbit teeth, showed higher enamel Mn/Ca (1 10^{-3} and 5.7 10^{-4}, respectively). The samples were noted to be "stained".
- Samples 35034 and 35035, two rabbit teeth, showed higher enamel Fe/Ca compared to other teeth (1.2 10^{-3} and 2.2 10^{-3}, respectively). The samples were noted to be "stained" and "normal".
- It should be noted that all the abovementioned rabbit teeth had the highest Cu content of all analyzed samples (Table S11).

As rabbits' tooth enamel is extremely difficult to sample because of their small tooth size, it is not surprising that soil contaminants could be present along with the enamel.

We also explore the correlations between those ratios and found several ones positively correlated:

Ratio 1	**Ratio 2**	**R^2**	p-value
Al/Ca	**Ba/Ca**	0.36	1.1 10^{-5}
Al/Ca	**Mn/Ca**	0.23	4.8 10^{-4}
Al/Ca	**Cu/Ca**	0.69	2.4 10^{-12}
Al/Ca	**Zn/Ca**	0.59	8.5 10^{-10}
Ba/Ca	**Zn/Ca**	0.4	3.8 10^{-6}
Cu/Ca	**Zn/Ca**	0.71	7.6 10^{-13}

Table S12. Element ratios for which a correlation was found in tooth enamel

There was no correlation with the $\%CO_3$ for all the element ratios, nor with the isotope ratios. Sr/Ca was not correlated to other ratios, including Ba/Ca.

If the five samples with elevated Mn, Al and Fe content (see section above) are removed, the correlations become what is described in the Table S13:

Ratio 1	Ratio 2	R^2	*p*-value	*p*-value<0.05
Al/Ca	**Ba/Ca**	0.01	0.25	NO
Al/Ca	**Mn/Ca**	0.03	0.15	NO
Al/Ca	**Fe/Ca**	0.33	$4.0\ 10^{-5}$	YES
Al/Ca	**Cu/Ca**	0.59	$2.1\ 10^{-8}$	YES
Al/Ca	**Zn/Ca**	0.42	$1.1\ 10^{-6}$	YES
Ba/Ca	**Zn/Ca**	0.003	0.75	NO
Cu/Ca	**Zn/Ca**	0.37	$3.9\ 10^{-4}$	YES
Fe/Ca	**Zn/Ca**	0.4	2.10^{-5}	YES

Table S13. Element ratios for which a correlation was found when diagenetic samples are removed.

When we compared the samples labeled “normal” to the samples “stained”, Kruskal Wallis test reveals that they are significantly different for all trace element ratios, except Sr/Ca:

Ratio 1	Median: Normal aspect	Median: Stained	chi-squared	*p*-value	*p*-value <0.05
Al/Ca	3.14 E-04	4.98 E-05	8.2	0.0042	YES
Ba/Ca	1.22 E-04	3.14 E-04	6.3	0.012	YES
Cu/Ca	6.50 E-06	3.05 E-05	7.7	0.0055	YES
Fe/Ca	1.76 E-05	5.44 E-05	9.8	0.0017	YES
Mn/Ca	3.36 E-05	2.08 E-04	12.4 [3]	0.0004	YES
Sr/Ca	6.09 E-04	8.83 E-04	2.6	0.1043	NO
Zn/Ca	1.70 E-04	3.25 E-04	7.4	0.0066	YES
%CO_3	6.85	8.36	4.3	0.0376	YES
$\delta^{18}O$ (‰)	-4.53	-4.08	0.8	0.3864	NO
$\delta^{13}C$ (‰)	-10.07	-9.81	0.03	0.8625	NO
$\delta^{66}Zn$ (‰)	1.14	1.08	3	0.0828	NO
$^{87}Sr/^{86}Sr$	0.70872	0.70859	2.9	0.0888	NO

Table S14. Chi-squared and p-value of Kruskal Wallis tests comparing various trace element and isotope ratios in teeth of normal aspect or stained.

None of the isotope ratios show statistically different values between the stained samples and the ones of regular aspect. This can partially be explained by the fact that they were sampled in a pristine area of the tooth, and none of them were stained, whereas trace element samples were taken afterward close to the first area sampled. Once the abovementioned outliers are removed, Al, Mn, Fe, and Cu content are in the same range as what is known for modern human and other animal teeth (44–48). Unlike Tacail et al. (2017), we observed that Zn/Ca and Cu/Ca ratios tend to be correlated even in the absence of potentially diagenetic samples. The correlation between Cu and Al also tends to persist. Other

correlations are much weaker and can be considered as not reliable. There is no content defined as a threshold showing the uptake of diagenetic components for Zn, Ba, and Sr content. However, their elemental abundances that we report are similar to those found in modern enamel (44).

3.3 Carbonate content

The non-diagenetic CO_3 content of enamel is usually below 10 % (49), and we decided to exclude all teeth (n=4/42) with an average %CO_3 higher than this amount when interpreting C and O isotope data (Table S16). The four excluded teeth were three rabbit teeth and one European wild ass tooth. However, the samples collected for Zn, trace elements, and Sr isotope analyses were taken separately, and we thus cannot fully compare diagenetic tracers for the different teeth. Nevertheless, we did not notice a higher Al, Fe, or Mn content in the four teeth excluded because of their more elevated % CO_3.

Finally, one dentin sample (34408) and one "dirty" (34409, that is to say with dark-colored cracks) enamel sample (both samples are wolf teeth) were analyzed to have an idea of the content of material more likely to be affected by diagenetic processes. They both showed a content of 12 % of CO_3, whereas the "clean" (that is to say without cracks) enamel sample had a content of 5 %. Their $\delta^{18}O$ values were clearly shifted towards lower values compared to the "clean" enamel, but the $\delta^{13}C$ values were shifted by only 0.5 ‰ in the "dirty" enamel. We acknowledge the limits of this comparison due to the low number of samples.

Supplementary Information 4

Supplementary information on Zn isotopic results and discussion

All Zn isotope ratios are given in Table S15 and shown in Figs. S6 and S7;

4.1 Statistical tests

- To adhere to parametric tests' assumptions, the Zn isotope dataset was examined for normally distributed data with a Shapiro Wilk test (W = 0.98, *p*-value = 0.67). However, many non-parametric tests, such as Kruskal-Wallis, were subsequently also used because of the small numbers of data per group (layer, species, tooth type, etc.).
- Zn isotope data are similar among the layers e, f and g (Kruskal-Wallis chi-squared = 5.16 df = 1, *p*-value = 0.16) (Figure S6)
- Zn isotope compositions are similar among different tooth types (Herbivores: Kruskal-Wallis chi-squared = 13.892, df = 8, p-value = 0.08461, Carnivores: Kruskal-Wallis chi-squared = 7.8876, df = 6, p-value = 0.2465)

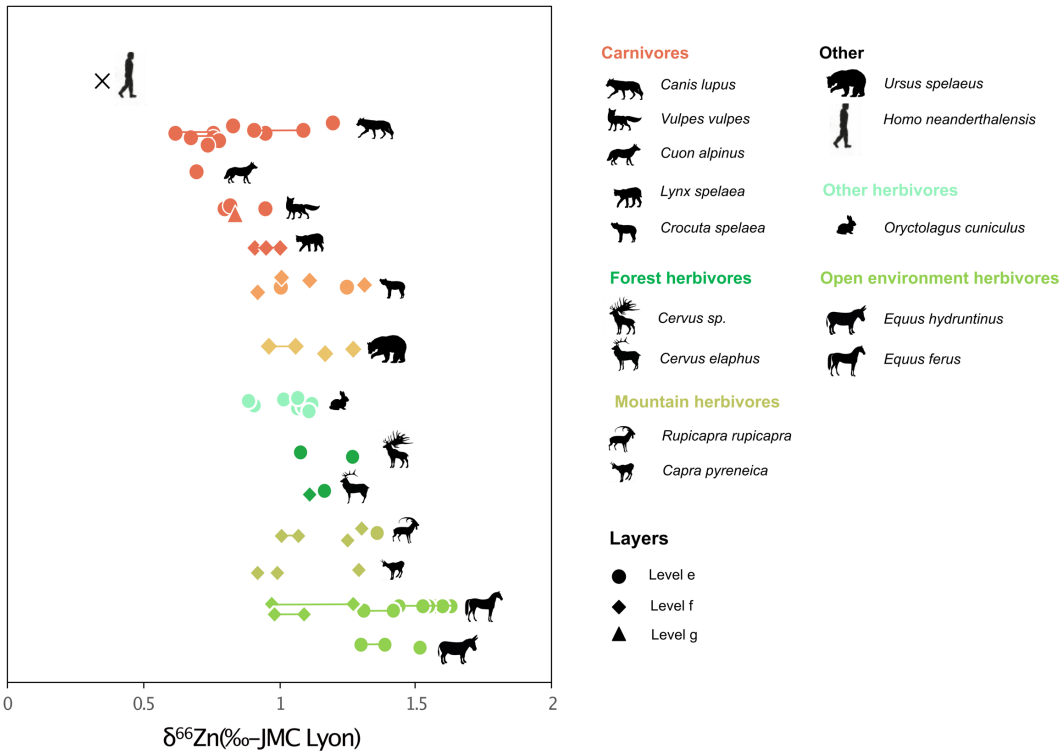

Figure S6: Zn isotope ratios in tooth enamel of animals from layers e, f and g in Gabasa, Spain. Each symbol represents one sample, but several samples were sometimes taken from the same tooth and a line binds them in this case (see also Table S15). See the Figure 2 and S7 to see the average values per individual. SD (<0.05 ‰) are also given but often smaller than the symbols. All data are here represented (the samples with elevated Al, Mn or Fe content are hence not excluded).

Id SEVA	Id museum	Species	Common name	Tooth	Tissue sampled	Number of samples taken from one tooth	Sample number	$\delta^{66}Zn$ (‰)	$1SD_{measurement}$	$1SD_{sample}$	Zn (ppm)	MC-ICPMS
34408	Ga1.2B.255.265	*Canis lupus*	Gray wolf	P4	enamel	3	1	0.95			77	Nu 500
					enamel		2	0.62			60	Neptune
					enamel		3	0.76			57	Neptune
							average value	0.78		0.17	64	
34409	Ga1.1C.217.13	*Canis lupus*	Gray wolf	M1 ?	enamel	2	1	1.09			43	Nu 500
					enamel		2	0.91			64	Neptune
							average value	1.00		0.13	54	
34410a	Ga1.5C.327.169	*Ursus* sp.	Bear	M2	enamel	1		1.27			43	Nu 500
34410b	Ga1.5C.348.546	*Ursus* sp.	Bear	M2	enamel	2	1	0.96			42	Neptune
					enamel		2	1.06			27	Neptune
							average value	1.01		0.07	35	
34411	Ga1.8B.205.103.(26)	*Crocuta* sp.	Hyena	M1 ?	enamel	2	1	1.01			75	Neptune
							2	1.25			91	Neptune
							average value	1.13		0.17	83	
34412	Ga1.5C.260.96	*Cuon* sp.	Dhole	P4 ?	enamel	1	1	0.70			59	Neptune
34413	Ga1.3A.263.49	*Rupicapra rupicapra*	Chamois	P3	enamel	2	1	1.07			*43*	Neptune
							2	1.01			44	Neptune
							average value	1.04		0.04	44	

Id SEVA	Id museum	Species	Common name	Tooth	Tissue sampled	Number of samples taken from one tooth	Sample number	$\delta^{66}Zn$ (‰)	$1SD_{measurement}$	$1SD_{sample}$	Zn (ppm)	MC-ICPMS
34414	Ga1.4A.239.75(96)	*Equus ferus*	Horse	P	enamel	7	1	1.63			*32*	Neptune
34414					enamel		2	1.44			26	Neptune
34414.1					enamel		3	1.57			49	Neptune Plus
34414.2					enamel		4	1.60			55	Neptune Plus
34414.3					enamel		5	1.54			51	Neptune Plus
34414.4					enamel		6	1.55			49	Neptune Plus
34414.5					enamel		7	1.53			72	Neptune Plus
							average value	1.55		0.06	48	
34415	GA15C.244.17	*Equus ferus*	Horse	P	enamel		1	1.42			36	Neptune
							2	1.31			33	Neptune
							average value	1.37		0.08	35	
34416	GA 1 3C.285.73	*Equus ferus*	Horse	P or M	enamel	1	1	1.27			24	Neptune
							2	0.97			23	Neptune
							average value	1.12		0.21	24	
34417	GA13A.285.89	*Cervus* sp.	Deer	M	enamel	1	1	1.11			33	Neptune
34418	Ga1.4C.177.116	*Equus hydruntinus*	European wild ass	P or M	enamel	2	1	1.30			38	Neptune
							2	1.39			28	Neptune
							average value	1.35		0.07	33	

Id SEVA	Id museum	Species	Common name	Tooth	Tissue sampled	Number of samples taken from one tooth	Sample number	$\delta^{66}Zn$ (‰)	$1SD_{measurement}$	$1SD_{sample}$	Zn (ppm)	MC-ICPMS
34419	GA1 4a 240.3 (19)	*Equus ferus*	Horse	P or M	enamel	2	1	1.09			33	Neptune
							2	0.98			24	Neptune
							average value	1.03		0.08	29	
34420	Ga1.3C.240	*Canis lupus*	Gray wolf	P4 ?	enamel	2	1	0.76			52	Neptune
							2	0.68			57	Neptune
							average value	0.72		0.05	54	
34421	Ga1.8B.210.70(51)	*Vulpes* sp.	Fox	P3	enamel	2	1	0.80			77	Neptune
							2	0.95			90	Neptune
							average value	0.88		0.11	84	
34422	Ga1 rev 303	*Homo neanderthalensis*	Neandertal	M1	enamel	1	1	0.35	0.00		111	Neptune
35034	rabbit e	*Oryctolagus cuniculus*	European rabbit	?	enamel	1	1	1.07			148	Neptune Plus
35035	rabbit e	*Oryctolagus cuniculus*	European rabbit	?	enamel	1	1	1.09	0.00		138	Neptune
35036	rabbit e	*Oryctolagus cuniculus*	European rabbit	?	enamel	1	1	0.91	0.00		119	Neptune
35037	rabbit e	*Oryctolagus cuniculus*	European rabbit	?	enamel	1	1	1.12	0.01		147	Neptune
35038	rabbit e	*Oryctolagus cuniculus*	European rabbit	?	enamel	1	1	0.89	0.00		184	Neptune

Id SEVA	Id museum	Species	Common name	Tooth	Tissue sampled	Number of samples taken from one tooth	Sample number	$\delta^{66}Zn$ (‰)	$1SD_{measurement}$	$1SD_{sample}$	Zn (ppm)	MC-ICPMS
35045	Ga1.6A.209.72	Cervid	Deer	M1	enamel	1	1	1.17	0.04		33	Neptune
35046	GA1-BA-230-220	*Canis* sp.	Gray wolf	P or M	enamel	1	1	0.83	0.01		34	Neptune
35047	GA1-BA-230-1B12	*Canis* sp.	Gray wolf	P or M	enamel	1	1	0.78	0.03		31	Neptune
35048	GA1-BA-225-310	*Canis* sp.	Gray wolf	P or M	enamel	1	1	0.74	0.02		49	Neptune
35049	Rabbit tooth E1	*Oryctolagus cuniculus*	European rabbit	?	enamel	1	1	1.02	0.02		105	Neptune
35050	Rabbit tooth E2	*Oryctolagus cuniculus*	European rabbit	?	enamel	1	1	1.11	0.02		116	Neptune
35051	Rabbit tooth E3	*Oryctolagus cuniculus*	European rabbit	?	enamel	1	1	1.07			82	Neptune
35052	GA15C.352.577	*Ursus* sp.	Bear	M2	enamel	1	1	1.17	0.00		36	Neptune
35053	Lib.289-198	*Capra pyreneica*	Ibex	M2	enamel	1	1	1.29	0.03		41	Neptune
35054.1	GA16B.245.119	*Capra pyreneica*	Ibex	M2	enamel	2	1	0.92	0.00		53	Neptune
							2	0.99	0.02		56	Neptune
							average value	0.96		0.05	54	
35055	GA18B.219.795-511	*Vulpes* sp.	Fox	p2	enamel	1	1	0.82	0.01		85	Neptune
35056	whole tooth lvl g	*Vulpes* sp.	Fox	dp4	enamel	1	1	0.84	0.00		90	Neptune

Id SEVA	Id museum	Species	Common name	Tooth	Tissue sampled	Number of samples taken from one tooth	Sample number	$\delta^{66}Zn$ (‰)	$1SD_{measurement}$	$1SD_{sample}$	Zn (ppm)	MC-ICPMS
35057.2	Ga11C.336.422	*Equus hydruntinus*	European wild ass	P or M	enamel	1	1	1.52	0.01		28	Neptune
					dentine	1	1	1.71	0.01		10	Neptune
					cementum	1	1	1.59	0.01		33	Neptune
35058.1	lynx	*Lynx spelaea*	Cave lynx	p4	enamel	3	1	0.91	0.01		55	
					enamel		2	1.00	0.01		80	Neptune
					enamel		3	0.95	0.01		76	Neptune
							average value	0.96		0.05	70	
35059	GA1B26.024 436	*Crocuta* sp.	Hyena	p3	enamel	1	1	1.31	0.01		62	Neptune
35060	GA1.6E.260.191	*Crocuta* sp.	Hyena	c	enamel	1	1	1.11	0.00		72	Neptune
35061	GA1.5B.282.42	*Crocuta* sp.	Hyena	c	enamel	1	1	1.01	0.03		54	Neptune
35062	GA16G2322960a	*Rupicapra rupicapra*	Chamois	m3	enamel	1	1	1.30	0.02		62	Neptune
35063	GA16G2322960b	*Rupicapra rupicapra*	Chamois	m3	enamel	1	1	1.25	0.02		67	Neptune
35064	Ga1.2B.235.125.67	*Cervus* sp.	Red deer	m1	enamel	1	1	1.27	0.01		44	Neptune
35065	Ga13B.290.82	*Cervus* sp.	Red deer	m2	enamel	1	1	1.08	0.04		28	Neptune
35066	GA1K.224.66	*Cervus* sp.	Gray wolf	p4	enamel	1	1	1.20			70	Neptune
35067	GA.7C.290.109	*Crocuta* sp.	Hyena	p3	enamel	1	1	0.92			49	Neptune

Id SEVA	Id museum	Species	Common name	Tooth	Tissue sampled	Number of samples taken from one tooth	Sample number	$\delta^{66}Zn$ (‰)	$1SD_{measurement}$	$1SD_{sample}$	Zn (ppm)	MC-ICPMS
35068	GA.16A.200.28	*Rupicapra rupicapra*	Chamois	m1/m2	enamel	1	1	1.36			59	Neptune

Table S15. Zn isotope and concentration results for the Gabasa teeth. Concentrations were analyzed on a Neptune ICP-MS using the protocol described in Jaouen et al. (2016)(32) derived from Copeland et al. (2008)(50). Depending on the sample, 1 to 7 preparations were performed (see column: Number of samples taken from one tooth and corresponding $\delta^{66}Zn_{enamel}$ values). Most $\delta^{66}Zn_{enamel}$ values correspond to one or two measurements, all analytical duplicates from a single aliquot had $\delta^{66}Zn_{enamel}$ values with SD < 0.05 ‰. The SD of the bracketing standard was between 0.02 and 0.05 ‰, depending on the session. Id S-EVA: Max Planck Institute for Evolutionary Anthropology identification number. Id museum: Huesca Museum identification number

4.2 Zn content of Gabasa mammal teeth

Zn concentrations are strongly zoned in tooth enamel (44, 45, 51). Indeed, the concentrations can vary substantially depending on the proportions of inner vs. outer enamel sampled. Here, Zn concentrations were estimated from two different samples for each tooth: one concentration was measured along with the Zn isotope ratios on the MC-ICP MS (and for some individuals, several samples were actually taken and measured within the same tooth, Table S15), and the other one along with other trace elements on the triple quadrupole ICP-MS. The Zn concentration measured on the ICP MS and the Zn/Ca ratios obtained from the triple quadrupole show a strong correlation of $R^2 = 0.69$ (p-value = $2.8\ 10^{-11}$). Concentrations estimated on the MC-ICP-MS (multicollector inductively coupled plasma mass spectrometer) for several samples from the same tooth also have the same order of magnitude. Despite the abovementioned bias, it seems that the measured concentrations are reliable. Therefore, we investigated the Zn content among the different taxa since an unusual pattern could reveal diagenetic uptake. The Zn concentration measured in tooth enamel appeared to be species-dependent (Kruskal-Wallis chi-squared = 37.014, df = 13, p-value = 0.0004122, test performed on the average value for each tooth) but also related to the dietary group (Kruskal-Wallis chi-squared = 29.858, df = 4, p-value = 0.000005232). Carnivores (including hyenas) have a median Zn concentration of 62 ppm, whereas ungulates coming from open environments have Zn concentrations around 30 ppm. Chamois and Iberian ibex have an intermediate median concentration of 54 ppm, while the Neandertal and rabbits have much higher Zn concentrations (median respectively at 111 and 128 ppm) (Figure S7). The higher concentration of Zn in primate tooth enamel compared to other mammals has already been reported in modern and archeological food webs. Higher Zn concentrations in carnivore teeth compared to ungulate are sometimes observed, but not systematically (28, 29, 44, 52), which could be explained by the abovementioned bias depending on the thickness of the enamel for the tooth and area sampled. There is only a single reference on Zn content in rabbit teeth, which also shows elevated amounts (around 200 ppm) (53). No physiological explanation has yet been provided for Zn content variability in different animal species.

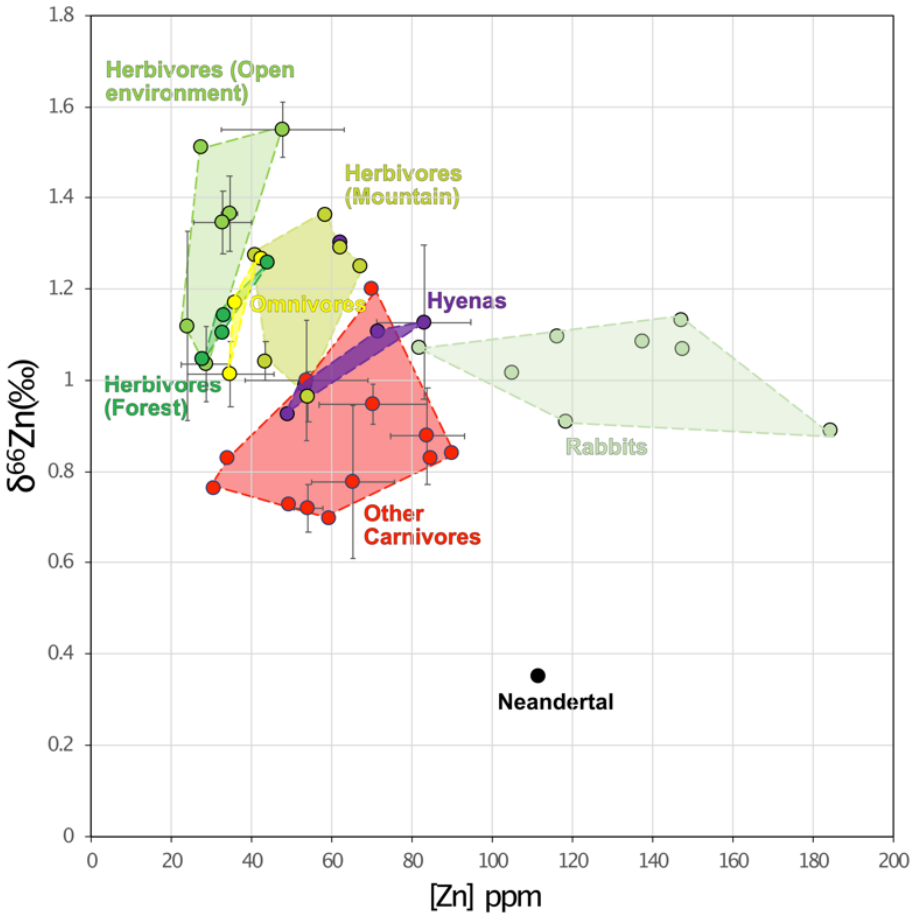

Figure S7. Enamel Zn content and isotope ratios in teeth of different dietary groups and species at Gabasa, Spain.

4.3 Zn isotope offsets between species or group of species

The trophic level spacing (TLS) for Zn isotope ratios has been observed to be between 0.3 and 0.6 ‰ (28–32). To establish the potential preys of carnivore at Gabasa, we looked at the offset between the mean $\delta^{66}Zn_{enamel}$ values of carnivores and herbivores (or groups of herbivores). Among others, we conclude that dholes (*C. alpinus*) were unlikely to feed on *E. hydruntinus* (TLS > 0.73 ‰, Table S16) and that bears (*Ursus* sp.) were mostly herbivores. Lynx (*L. spelaea*) which are supposed to feed on rabbits show an offset of 0.12‰. This small offset can be explained by the fact that they also digest a significant part of their bones, enriched in heavy Zn isotopes (54). One should notice that even the smallest offsets between the Neandertal and any herbivores (i.e., 0.68 ‰ between Neandertal' and rabbits' $\delta^{66}Zn_{enamel}$ values) are larger than the known TLS range.

Zooarchaeological data documents carnivore modifications on caprid bones, which is consistent with the offsets of 0.3‰. However, small-sized carnivores are unlikely to have transported the ungulates found in the cave (14). Deer, equids, and Iberian ibex are preyed upon by the medium-sized carnivores (wolves and hyenas) (14)

	Bear	Chamois	Deer	Wild ass	Horse	Rabbit	Ibex	Herbivores	Mountain	Forest	Open
Bear		0.09	0.01	0.28	0.15	-0.12	-0.02	0.05	0.05	0.01	0.20
Dhole	0.45	0.54	0.46	0.73	0.60	0.33	0.43	0.50	0.50	0.46	0.65
Fox	0.30	0.39	0.31	0.59	0.46	0.18	0.28	0.35	0.35	0.31	0.50
Hyena	0.05	0.14	0.06	0.34	0.21	-0.07	0.03	0.10	0.10	0.06	0.25
Lynx	0.24	0.33	0.25	0.52	0.39	0.12	0.22	0.29	0.29	0.25	0.44
Neandertal	0.80	0.88	0.81	1.08	0.95	0.68	0.78	0.85	0.85	0.81	1.00
Wolf	0.28	0.37	0.29	0.57	0.44	0.16	0.26	0.33	0.33	0.29	0.48

Table S16. Average $\delta^{66}Zn_{enamel}$ offsets between species or group of species (classified by type of environments according to Blasco (1995)). The two rabbit teeth with elevated trace element content were excluded. These offsets can be compared to the trophic level spacing of 0.3 to 0.6 ‰.

Day of analysis	Id ARCH	Id SEVA	Species	Tissue	$^{87}Sr/^{86}Sr_{uncorr}$	$^{87}Sr/^{86}Sr_{corr}$ [1]	err std (SE)	SD [2]	Measured with
03/03/2020	ARCH 82	Sr 34414.1	*Equus ferus*	enamel	0.708851	0.708811	6.6E-06		Triton Plus
03/03/2020	ARCH 83	Sr 34414.2	*Equus ferus*	enamel	0.708828	0.708788	1.0E-05		Triton Plus
04/03/2020	ARCH 84	Sr 34414.3	*Equus ferus*	enamel	0.708804	0.708764	7.4E-06		Triton Plus
04/03/2020	ARCH 85	Sr 34414.4	*Equus ferus*	enamel	0.708741	0.708701	8.7E-06		Triton Plus
04/03/2020	ARCH 86	Sr 34417	*Cervus elaphus*	enamel	0.708628	0.708588	1.3E-05		Triton Plus
04/03/2020	ARCH 87	Sr 34418	*Equus hydrontinus*	enamel	0.709157	0.709117	8.3E-06		Triton Plus
04/03/2020	ARCH 88	Sr 35034	*Oryctolagus cuniculus*	enamel	0.708637	0.708597	1.5E-05		Triton Plus
04/03/2020	ARCH 89	Sr 35035	*Oryctolagus cuniculus*	enamel	0.708588	0.708548	1.5E-05		Triton Plus
04/03/2020	ARCH 90	Sr 35036	*Oryctolagus cuniculus*	enamel	0.708770	0.708730	1.2E-05		Triton Plus
04/03/2020	ARCH 91	Sr 35037	*Oryctolagus cuniculus*	enamel	0.708625	0.708585	7.6E-06		Triton Plus
05/03/2020	ARCH 92	Sr 35038	*Oryctolagus cuniculus*	enamel	0.708726	0.708686	3.1E-05		Triton Plus
05/03/2020	ARCH 93	Sr 35057	*Equus hydrontinus*	enamel	0.709149	0.709109	9.4E-06		Triton Plus
05/03/2020	ARCH 94	Sr 35059	*Crocuta* sp.	enamel	0.708791	0.708751	5.1E-06		Triton Plus
27/05/2020	ARCH 95	Sr 34414.5	*Equus ferus*	enamel	0.708690	0.708650	1.1E-05		Triton Plus
27/05/2020	ARCH 96	Sr 34045	*Cervid*	enamel	0.708641	0.708601	1.1E-05		Triton Plus
27/05/2020	ARCH 97	Sr 34053	*Capra pyreneica*	enamel	0.708764	0.708724	3.5E-06		Triton Plus
27/05/2020	ARCH 98	Sr 35061	*Crocuta* sp.	enamel	0.708760	0.708720	9.6E-06		Triton Plus
27/05/2020	ARCH 99	Sr 35067	*Crocuta* sp.	enamel	0.708522	0.708482	9.7E-06		Triton Plus
31/05/2021	ARCH 78	Sr 34408	*Canis lupus*	enamel	0.708342	0.708319	3.5E-05	4.6E-05	Neptune Plus and Nu 500
31/05/2021	ARCH 79	Sr 34409	*Canis lupus*	enamel	0.708739	0.708715	1.3E-05	1.2E-05	Neptune Plus and Nu 500
31/05/2021	ARCH 80	Sr 34422	*Homo neanderthalensis*	enamel	0.708601	0.708553	2.6E-05	1.5E-04	Neptune Plus and Nu 500
31/05/2021	ARCH 78	Sr 34408	*Canis lupus*	dentine	0.708355	0.708344	2.3E-05		Neptune Plus
31/05/2021	ARCH 79	Sr 34409	*Canis lupus*	dentine	0.708580	0.708568	1.4E-05		Neptune Plus
11/09/2018	NA	Sr 34413	*Rupicapra rupicapra*	enamel	0.708435	0.708381	5.0E-06		Neptune

Table S17. Sr isotope ratios in tooth material of Gabasa mammals. Id ARCH: Identification number related to the ERC ARCHEIS project at Géosciences Environnement Toulouse, Id SEVA: Identification number at the Max Planck Institute for Evolutionary Anthropology. See text for the details on the correction. [1.] 3 samples were both analyzed on a Neptune Plus and a Nu500. The ratios given in this list are those analyzed on the Neptune Plus. [2.] SD between the measurements on the Neptune Plus and the Nu 500

Supplementary Information 5

Supplementary information on Sr isotopic results and discussion

All Sr isotope ratios are given in Table S18.

Strontium isotope analyses were conducted on 24 enamel samples belonging to 21 different animals from 9 species (2 wolves, 3 hyenas, 1 Neandertal and 15 different herbivores). In addition, two Sr isotope analyses were conducted on the dentin of the two different wolves. We compiled all Sr isotope data available for rocks of the Ebro Valley area to obtain the local baseline (Figure S8), for which the average ratio is 0.7086 ± 0.0038 1 SD (n = 146, Table S18), which is extremely close to the average $^{87}Sr/^{86}Sr$ observed among Gabasa's mammals (0.70869 ± 0.00018, 1SD). The data compiled are listed in the Table S18 with the associated references (3–10, 55). The Sr isotope ratios of Gabasa teeth are compatible with the local Cretaceous, Miocene and Paleocene lithologies. The enamel values have similar ratios in comparison to the dentin values, more prone to be overprinted by soil contaminants (0.70844 ± 0.00016 1SD).

Country	Lat	Long	Region	Site	Geological age	Sample type	$^{87}Sr/^{86}Sr$	Reference
Spain	NA	NA	Pyrenean	Ebro Basin, close to San Juan cave	Cretaceous Miocene	Rabbit tooth	0.7090	Villalba-Mouco et al. (2018)
Spain	NA	NA	Pyrenean	Ebro Basin, close to San Juan cave	Cretaceous Miocene	Rabbit tooth	0.7087	Villalba-Mouco et al. (2018)
Spain	NA	NA	Pyrenean	Ebro Basin, close to San Juan cave	Cretaceous Miocene	Rabbit tooth	0.7089	Villalba-Mouco et al. (2018)
Spain	NA	NA	Pyrenean	Ebro Basin, close to San Juan cave	Cretaceous Miocene	Rabbit tooth	0.7085	Villalba-Mouco et al. (2018)
Spain	NA	NA	Pyrenean	Ebro Basin, close to San Juan cave	Continental Paleogene	snail	0.7080	Villalba-Mouco et al. (2018)
Spain	NA	NA	Pyrenean	Ebro Basin, close to San Juan cave	Continental Paleogene	snail	0.7080	Villalba-Mouco et al. (2018)
Spain	NA	NA	Pyrenean	Ebro Basin, close to San Juan cave	Continental Paleogene	snail	0.7081	Villalba-Mouco et al. (2018)
Spain	NA	NA	Pyrenean	Ebro Basin, close to San Juan cave	Continental Paleogene	snail	0.7080	Villalba-Mouco et al. (2018)
Spain	NA	NA	Pyrenean	Ebro Basin, close to San Juan cave	Continental Paleogene	snail	0.7082	Villalba-Mouco et al. (2018)
Spain	NA	NA	Pyrenean	Ebro Basin, close to San Juan cave	Continental Paleogene	grass	0.7083	Villalba-Mouco et al. (2018)
Spain	NA	NA	Pyrenean	Ebro Basin, close to San Juan cave	Continental Paleogene	bush	0.7082	Villalba-Mouco et al. (2018)
Spain	NA	NA	Pyrenean	Ebro Basin, close to San Juan cave	Continental Paleogene	tree	0.7083	Villalba-Mouco et al. (2018)
Spain	NA	NA	Pyrenean	Ebro Basin, close to San Juan cave	Continental Paleogene	bush	0.7083	Villalba-Mouco et al. (2018)
Spain	NA	NA	Pyrenean	Ebro Basin, close to San Juan cave	Continental Paleogene	bush	0.7081	Villalba-Mouco et al. (2018)
Spain	NA	NA	Pyrenean	Cantabrian mountains	Trias	Carbonate	0.7078	Sopena et al. (2009)

Country	Lat	Long	Region	Site	Geological age	Sample type	$^{87}Sr/^{86}Sr$	Reference
Spain	NA	NA	Pyrenean	Cantabrian mountains	Trias	Carbonate	0.7078	Sopena et al. (2009)
Spain	42.2127780	2.490278	Pyrenean	see coordinates	NA	NA	0.7084	Hoogewerff et al. (2019)
Spain	NA	NA	Pyrenean	Serra del Montsec	Coniacian–Santonian	rudist	0.7074	Boix et al. (2011)
Spain	NA	NA	Pyrenean	Serra del Montsec	Coniacian–Santonian	rudist	0.7074	Boix et al. (2011)
Spain	NA	NA	Pyrenean	Serra del Montsec	Coniacian–Santonian	rudist	0.7074	Boix et al. (2011)
Spain	NA	NA	Pyrenean	Serra del Montsec	Coniacian–Santonian	rudist	0.7074	Boix et al. (2011)
Spain	NA	NA	Pyrenean	Serra del Montsec	Coniacian–Santonian	rudist	0.7074	Boix et al. (2011)
Spain	NA	NA	Pyrenean	Serra del Montsec	Coniacian–Santonian	rudist	0.7074	Boix et al. (2011)
Spain	NA	NA	Pyrenean	Serra del Montsec	Coniacian–Santonian	rudist	0.7074	Boix et al. (2011)
Spain	NA	NA	Pyrenean	Serra del Montsec	Coniacian–Santonian	rudist	0.7074	Boix et al. (2011)
Spain	NA	NA	Pyrenean	Serra del Montsec	Coniacian–Santonian	rudist	0.7074	Boix et al. (2011)
Spain	NA	NA	Pyrenean	Serra del Montsec	Coniacian–Santonian	rudist	0.7074	Boix et al. (2011)
Spain	NA	NA	Pyrenean	Serra del Montsec	Coniacian–Santonian	rudist	0.7075	Boix et al. (2011)
Spain	NA	NA	Pyrenean	Serra del Montsec	Coniacian–Santonian	rudist	0.7074	Boix et al. (2011)
Spain	NA	NA	Pyrenean	Serra del Montsec	Coniacian–Santonian	rudist	0.7074	Boix et al. (2011)
Spain	NA	NA	Pyrenean	Serra del Montsec	Coniacian–Santonian	rudist	0.7073	Boix et al. (2011)
Spain	NA	NA	Pyrenean	Serra del Montsec	Coniacian–Santonian	rudist	0.7074	Boix et al. (2011)
Spain	NA	NA	Pyrenean	Serra del Montsec	Coniacian–Santonian	rudist	0.7074	Boix et al. (2011)
Spain	NA	NA	Pyrenean	Serra del Montsec	Coniacian–Santonian	rudist	0.7074	Boix et al. (2011)
Spain	NA	NA	Pyrenean	Serra del Montsec	Coniacian–Santonian	rudist	0.7074	Boix et al. (2011)
Spain	NA	NA	Pyrenean	Serra del Montsec	Coniacian–Santonian	rudist	0.7074	Boix et al. (2011)
Spain	NA	NA	Pyrenean	Serra del Montsec	Coniacian–Santonian	rudist	0.7074	Boix et al. (2011)
Spain	NA	NA	Pyrenean	Serra del Montsec	Coniacian–Santonian	rudist	0.7073	Boix et al. (2011)
Spain	NA	NA	Pyrenean	Serra del Montsec	Coniacian–Santonian	rudist	0.7074	Boix et al. (2011)
Spain	NA	NA	Pyrenean	Serra del Montsec	Coniacian–Santonian	rudist	0.7077	Boix et al. (2011)
Spain	NA	NA	Pyrenean	central South Pyrenees	Late Cretaceous	bivalve	0.7077	Caus et al. (2016)
Spain	NA	NA	Pyrenean	central South Pyrenees	Late Cretaceous	bivalve	0.7077	Caus et al. (2016)
Spain	NA	NA	Pyrenean	central South Pyrenees	Late Cretaceous	bivalve	0.7077	Caus et al. (2016)
Spain	NA	NA	Pyrenean	central South Pyrenees	Late Cretaceous	matrix	0.7078	Caus et al. (2016)
Spain	NA	NA	Pyrenean	central South Pyrenees	Late Cretaceous	ostreid	0.7077	Caus et al. (2016)
Spain	NA	NA	Pyrenean	central South Pyrenees	Late Cretaceous	ostreid	0.7077	Caus et al. (2016)
Spain	NA	NA	Pyrenean	central South Pyrenees	Late Cretaceous	ostreid	0.7077	Caus et al. (2016)
Spain	NA	NA	Pyrenean	central South Pyrenees	Late Cretaceous	ostreid	0.7077	Caus et al. (2016)
Spain	NA	NA	Pyrenean	central South Pyrenees	Late Cretaceous	rudist	0.7077	Caus et al. (2016)
Spain	NA	NA	Pyrenean	central South Pyrenees	Late Cretaceous	rudist	0.7077	Caus et al. (2016)
Spain	NA	NA	Pyrenean	central South Pyrenees	Late Cretaceous	rudist	0.7077	Caus et al. (2016)

Country	Lat	Long	Region	Site	Geological age	Sample type	$^{87}Sr/^{86}Sr$	Reference
Spain	NA	NA	Pyrenean	central South Pyrenees	Late Cretaceous	rudist	0.7077	Caus et al. (2016)
Spain	NA	NA	Pyrenean	central South Pyrenees	Late Cretaceous	rudist	0.7077	Caus et al. (2016)
Spain	NA	NA	Pyrenean	central South Pyrenees	Late Cretaceous	matrix	0.7078	Caus et al. (2016)
Spain	NA	NA	Pyrenean	central South Pyrenees	Late Cretaceous	rudist	0.7077	Caus et al. (2016)
Spain	NA	NA	Pyrenean	central South Pyrenees	Late Cretaceous	rudist	0.7077	Caus et al. (2016)
Spain	NA	NA	Pyrenean	central South Pyrenees	Late Cretaceous	rudist	0.7077	Caus et al. (2016)
Spain	NA	NA	Pyrenean	Upper Cretaceous Terradets Limestone	middle Campanian	rudist	0.7076	Villalonga et al. (2019)
Spain	NA	NA	Pyrenean	Upper Cretaceous Terradets Limestone	middle Campanian	rudist	0.7076	Villalonga et al. (2019)
Spain	NA	NA	Pyrenean	Upper Cretaceous Terradets Limestone	middle Campanian	rudist	0.7076	Villalonga et al. (2019)
Spain	NA	NA	Pyrenean	Upper Cretaceous Terradets Limestone	middle Campanian	rudist	0.7076	Villalonga et al. (2019)
Spain	NA	NA	Pyrenean	Upper Cretaceous Terradets Limestone	middle Campanian	rudist	0.7075	Villalonga et al. (2019)
Spain	NA	NA	Pyrenean	Upper Cretaceous Terradets Limestone	middle Campanian	rudist	0.7075	Villalonga et al. (2019)
Spain	NA	NA	Pyrenean	Southern Pyrenees	Eocene	Calcite	0.7079	Travé et al. (1996)
Spain	NA	NA	Pyrenean	Southern Pyrenees	Eocene	Calcite	0.7079	Travé et al. (1996)
Spain	NA	NA	Pyrenean	Southern Pyrenees	Eocene	Calcite	0.7082	Travé et al. (1996)
Spain	NA	NA	Pyrenean	Southern Pyrenees	Eocene	Calcite	0.7082	Travé et al. (1996)
Spain	NA	NA	Pyrenean	Southern Pyrenees	Eocene	Calcite	0.7093	Travé et al. (1996)
Spain	NA	NA	Pyrenean	Southern Pyrenees	Eocene	Calcite	0.7092	Travé et al. (1996)
Spain	NA	NA	Pyrenean	Southern Pyrenees	Eocene	Calcitic marl	0.7079	Travé et al. (1996)
Spain	NA	NA	Pyrenean	Southern Pyrenees	Eocene	Calcitic marl	0.7079	Travé et al. (1996)
Spain	NA	NA	Pyrenean	Southern Pyrenees	Eocene	Celestite	0.7077	Travé et al. (1996)
Spain	NA	NA	Pyrenean	Southern Pyrenees	Eocene	Celestite	0.7079	Travé et al. (1996)
Spain	NA	NA	Pyrenean	Southern Pyrenees	Eocene	Celestite	0.7079	Travé et al. (1996)
Spain	NA	NA	Pyrenean	Southern Pyrenees	Eocene	Celestite	0.7079	Travé et al. (1996)
Spain	NA	NA	Pyrenean	Southern Pyrenees	Eocene	Celestite	0.7080	Travé et al. (1996)
Spain	42.728889	-1.301111	Pyrenean	see coordinates	NA	NA	0.7084	Hoogewerff et al. (2019)
Spain	42.7283299	-1.2997174	Pyrenean	see coordinates	NA	NA	0.7082	Hoogewerff et al. (2019)
Spain	42.7319425	-0.749445	Pyrenean	see coordinates	NA	NA	0.7083	Hoogewerff et al. (2019)
Spain	42.4336129	0.07249572	Pyrenean	see coordinates	NA	NA	0.7079	Hoogewerff et al. (2019)
Spain	42.4338890	0.072778	Pyrenean	see coordinates	NA	NA	0.7084	Hoogewerff et al. (2019)
Spain	NA	NA	Pyrenean	Southern Pyrenees	Eocene	bulk marl	0.7099	Travé et al. (1996)

Country	Lat	Long	Region	Site	Geological age	Sample type	$^{87}Sr/^{86}Sr$	Reference
Spain	NA	NA	Pyrenean	Southern Pyrenees	Eocene	bulk marl	0.7098	Travé et al. (1996)
Spain	NA	NA	Pyrenean	Southern Pyrenees	Eocene	Siliciclastic marl	0.7172	Travé et al. (1996)
Spain	NA	NA	Pyrenean	Southern Pyrenees	Eocene	Siiciclastic marl	0.7144	Travé et al. (1996)
Spain	NA	NA	Pyrenean	Southern Pyrenees	Eocene	Siliciclaastic marl	0.7189	Travé et al. (1996)
Spain	42.6013931	-1.869168	Pyrenean	see coordinates	NA	NA	0.7081	Hoogewerff et al. (2019)
Spain	42.2561110	-1.802500	Pyrenean	see coordinates	NA	NA	0.7085	Hoogewerff et al. (2019)
Spain	41.6400000	1.349167	Pyrenean	see coordinates	NA	NA	0.7083	Hoogewerff et al. (2019)
Spain	41.6405563	1.350282	Pyrenean	see coordinates	NA	NA	0.7083	Hoogewerff et al. (2019)
Spain	42.2147233	2.4858374	Pyrenean	see coordinates	NA	NA	0.7079	Hoogewerff et al. (2019)
Spain	NA	NA	Pyrenean	Vallès-Penedès half-graben	Early Miocene	Calcite	0.7134	Travé Calvet (2001)
Spain	NA	NA	Pyrenean	Vallès-Penedès half-graben	Early Miocene	Calcite	0.7136	Travé Calvet (2001)
Spain	NA	NA	Pyrenean	Vallès-Penedès half-graben	Early Miocene	Calcite	0.7136	Travé Calvet (2001)
Spain	NA	NA	Pyrenean	Vallès-Penedès half-graben	Early Miocene	Calcite	0.7135	Travé Calvet (2001)
Spain	NA	NA	Pyrenean	Vallès-Penedès half-graben	Early Miocene	Calcite	0.7130	Travé Calvet (2001)
Spain	NA	NA	Pyrenean	Vallès-Penedès half-graben	Early Miocene	Calcite	0.7114	Travé Calvet (2001)
Spain	NA	NA	Pyrenean	Vallès-Penedès half-graben	Early Miocene	Calcite	0.7134	Travé Calvet (2001)
Spain	NA	NA	Pyrenean	Vallès-Penedès half-graben	Early Miocene	Calcite	0.7109	Travé Calvet (2001)
Spain	NA	NA	Pyrenean	Vallès-Penedès half-graben	Early Miocene	Calcite	0.7135	Travé Calvet (2001)
Spain	NA	NA	Pyrenean	Vallès-Penedès half-graben	Early Miocene	Lime	0.7078	Negrel et al. (2017)
Spain	NA	NA	Pyrenean	Vallès-Penedès half-graben	Early Miocene	Lime	0.7092	Negrel et al. (2017)
Spain	NA	NA	Pyrenean	Vallès-Penedès half-graben	Early Miocene	Lime	0.7082	Negrel et al. (2017)
Spain	NA	NA	Pyrenean	Vallès-Penedès half-graben	Early Miocene	Lime	0.7086	Negrel et al. (2017)
Spain	42.2808370	-1.182495	Pyrenean	see coordinates	NA	NA	0.7084	Hoogewerff et al. (2019)
Spain	41.4647243	-0.3863936	Pyrenean	see coordinates	NA	NA	0.7081	Hoogewerff et al. (2019)
Spain	41.4644440	-0.385000	Pyrenean	see coordinates	NA	NA	0.7081	Hoogewerff et al. (2019)
Spain	41.5630563	0.758895	Pyrenean	see coordinates	NA	NA	0.7092	Hoogewerff et al. (2019)
Spain	NA	NA	Pyrenean	Ebro Basin, close to San Juan cave	Cretaceous Miocene	snail	0.7089	Villalba-Mouco et al. (2018)
Spain	NA	NA	Pyrenean	Ebro Basin, close to San Juan cave	Cretaceous Miocene	snail	0.7083	Villalba-Mouco et al. (2018)
Spain	NA	NA	Pyrenean	Ebro Basin, close to San Juan cave	Cretaceous Miocene	snail	0.7087	Villalba-Mouco et al. (2018)
Spain	NA	NA	Pyrenean	Ebro Basin, close to San Juan cave	Cretaceous Miocene	snail	0.7083	Villalba-Mouco et al. (2018)
Spain	NA	NA	Pyrenean	Ebro Basin, close to San Juan cave	Cretaceous Miocene	snail	0.7082	Villalba-Mouco et al. (2018)
Spain	NA	NA	Pyrenean	Ebro Basin, close to San Juan cave	Cretaceous Miocene	grass	0.7100	Villalba-Mouco et al. (2018)
Spain	NA	NA	Pyrenean	Ebro Basin, close to San Juan cave	Cretaceous Miocene	bush	0.7083	Villalba-Mouco et al. (2018)

Country	Lat	Long	Region	Site	Geological age	Sample type	$^{87}Sr/^{86}Sr$	Reference
Spain	NA	NA	Pyrenean	Ebro Basin, close to San Juan cave	Cretaceous Miocene	tree	0.7089	Villalba-Mouco et al. (2018)
Spain	NA	NA	Pyrenean	Ebro Basin, close to San Juan cave	Cretaceous Miocene	bush	0.7083	Villalba-Mouco et al. (2018)
Spain	NA	NA	Pyrenean	Ebro Basin, close to San Juan cave	Cretaceous Miocene	bush	0.7084	Villalba-Mouco et al. (2018)
Spain	NA	NA	Pyrenean	Ebro Basin, close to San Juan cave	Cretaceous Miocene	tooth	0.7085	Villalba-Mouco et al. (2018)
Spain	42.4616670	0.622778	Pyrenean	see coordinates	NA	NA	0.7141	Hoogewerff et al. (2019)
Spain	NA	NA	Pyrenean	Gabasa	Quaternary/Tertiary	animal teeth	0.7088	This study
Spain	NA	NA	Pyrenean	Gabasa	Quaternary/Tertiary	animal teeth	0.7088	This study
Spain	NA	NA	Pyrenean	Gabasa	Quaternary/Tertiary	animal teeth	0.7088	This study
Spain	NA	NA	Pyrenean	Gabasa	Quaternary/Tertiary	animal teeth	0.7087	This study
Spain	NA	NA	Pyrenean	Gabasa	Quaternary/Tertiary	animal teeth	0.7086	This study
Spain	NA	NA	Pyrenean	Gabasa	Quaternary/Tertiary	animal teeth	0.7091	This study
Spain	NA	NA	Pyrenean	Gabasa	Quaternary/Tertiary	animal teeth	0.7091	This study
Spain	NA	NA	Pyrenean	Gabasa	Quaternary/Tertiary	animal teeth	0.7086	This study
Spain	NA	NA	Pyrenean	Gabasa	Quaternary/Tertiary	animal teeth	0.7085	This study
Spain	NA	NA	Pyrenean	Gabasa	Quaternary/Tertiary	animal teeth	0.7087	This study
Spain	NA	NA	Pyrenean	Gabasa	Quaternary/Tertiary	animal teeth	0.7086	This study
Spain	NA	NA	Pyrenean	Gabasa	Quaternary/Tertiary	animal teeth	0.7087	This study
Spain	NA	NA	Pyrenean	Gabasa	Quaternary/Tertiary	animal teeth	0.7083	This study
Spain	NA	NA	Pyrenean	Gabasa	Quaternary/Tertiary	animal teeth	0.7088	This study
Spain	NA	NA	Pyrenean	Western Pyrenees	Lat Cretaceous	NA	0.7078	Sarasketa-Gartzia et al. (2018)
Spain	NA	NA	Pyrenean	Western Pyrenees	Late Cretaceous	NA	0.7080	Sarasketa-Gartzia et al. (2018)
Spain	NA	NA	Pyrenean	Western Pyrenees	Late Cretaceous	conglomerate sandstone clay limestone	0.7112	Sarasketa-Gartzia et al. (2018)
Spain	NA	NA	Pyrenean	Western Pyrenees	Late Cretaceous	NA	0.7074	Sarasketa-Gartzia et al. (2018)
Spain	NA	NA	Pyrenean	Western Pyrenees	Late Cretaceous	NA	0.7038	Sarasketa-Gartzia et al. (2018)
Spain	NA	NA	Pyrenean	Western Pyrenees	Late Cretaceous	NA	0.7054	Sarasketa-Gartzia et al. (2018)
Spain	NA	NA	Pyrenean	Western Pyrenees	Late Cretaceous	conglomerate sandstone clay limestone	0.7078	Sarasketa-Gartzia et al. (2018)
Spain	NA	NA	Pyrenean	Western Pyrenees	Late Cretaceous	conglomerate sandstone clay limestone	0.7079	Sarasketa-Gartzia et al. (2018)
Spain	NA	NA	Pyrenean	Western Pyrenees	Late Cretaceous	conglomerate sandstone clay limestone	0.7078	Sarasketa-Gartzia et al. (2018)
Spain	NA	NA	Pyrenean	Western Pyrenees	Late Cretaceous	conglomerate sandstone clay limestone	0.7080	Sarasketa-Gartzia et al. (2018)

Country	Lat	Long	Region	Site	Geological age	Sample type	$^{87}Sr/^{86}Sr$	Reference
Spain	NA	NA	Pyrenean	Western Pyrenees	Late Cretaceous	limestone and marls	0.7077	Sarasketa-Gartzia et al. (2018)
Spain	NA	NA	Pyrenean	Western Pyrenees	Late Cretaceous	limestone and marls	0.7080	Sarasketa-Gartzia et al. (2018)

Table S18 Strontium isotope data of different environmental samples from areas close to Gabasa deriving from different Mesozoic and Cenozoic bedrocks.(3–10, 55)

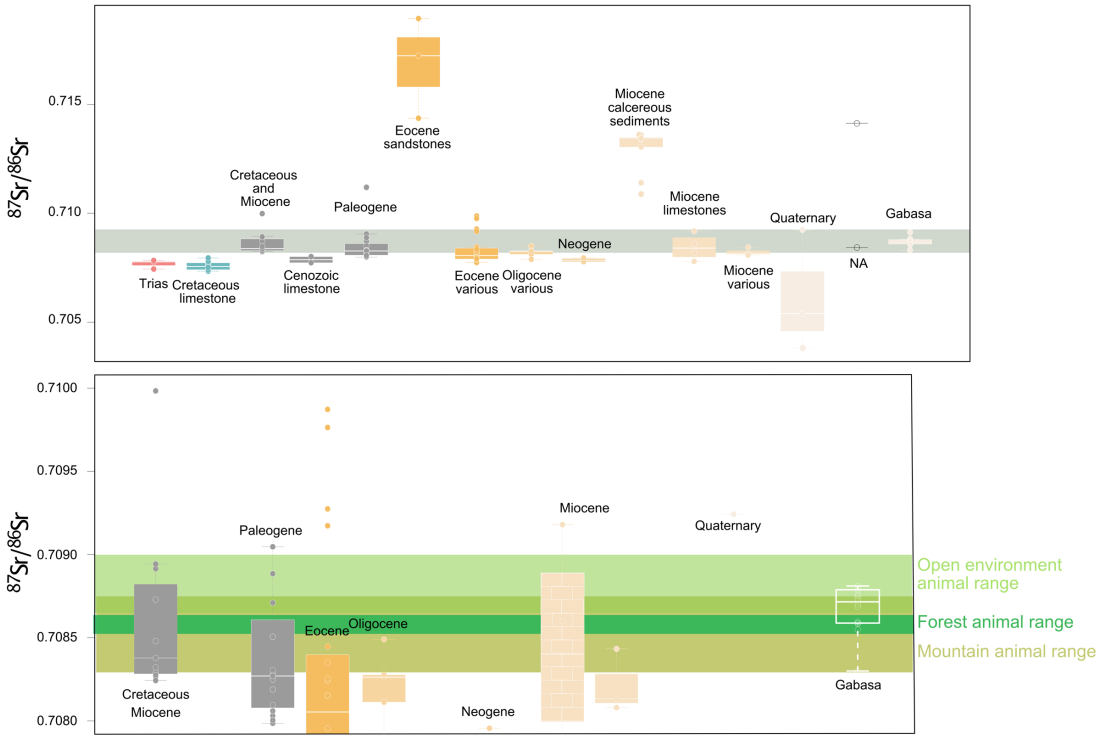

Figure S8. Strontium isotope ratios of different lithologies in the region of Gabasa. Upper panel: all data. The gray area corresponds to the range observed at Gabasa in mammals' teeth. Lower panel: data ranging between 0.7079 and 0.7100.

We do not observe a clear association between Sr isotope ratios and the ecology of the herbivores, but the tooth enamel of the two European wild asses shows the highest values (Figure S9). It is hard to determine the precise geographical origin of those equids, but it can be excluded that they were feeding on Triassic and Cretaceous regions. They were most likely feeding on the Eocene and Paleogene soils from lower altitudes. The Neandertal individual shows a ratio (0.70855) very close to the average Sr isotope average value, which is consistent with being local.

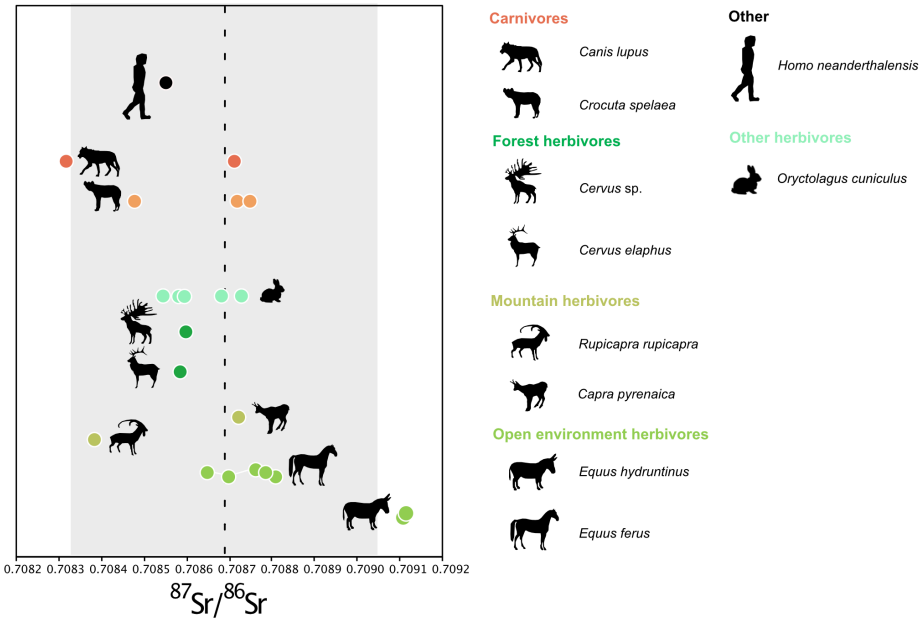

Figure S9. Strontium isotope ratios in dental enamel of Gabasa mammals. The gray area corresponds to 2 SD above and below the average Sr isotope values in Gabasa mammals' dental enamel. All horse values are from serial-samples within the same tooth.

Supplementary Information 6

Supplementary information on C and O isotopic results and discussion

All C and O isotope ratios are given in the Table S19.

Sample ID	sample size (µg)	$\delta^{13}C$ (‰) PDB	$\delta^{18}O$ (‰) PDB	carbonate content (%)	Average $\delta^{13}C$ (‰) PDB	Average $\delta^{18}O$ (‰) PDB	Average carbonate content (%)	Standard deviation $\delta^{13}C$ (‰) PDB	Standard deviation $\delta^{18}O$ (‰) PDB	Standard deviation carboante content (%)	Species
34410	90	-13.31	-6.50	7							
	88	-13.28	-6.33	7	**-13.30**	**-6.42**	**7**	0.02	0.12	<1	*Ursus* sp.
34411	91	-12.45	-4.52	7							
	99	-12.50	-4.69	7	**-12.47**	**-4.61**	**7**	0.04	0.13	<1	*Crocuta* sp.
34412	86	-11.27	-3.54	8							
	79	-11.32	-3.40	8	**-11.29**	**-3.47**	**8**	0.04	0.10	<1	*Cuon* sp.
34413	70	-10.09	-3.59	8							
	87	-10.33	-3.46	9	**-10.21**	**-3.53**	**8**	0.17	0.10	<1	*Rupicapra rupicapra*
34414.1	81	-9.17	-5.77	8							
	76	-9.35	-5.97	8	**-9.26**	**-5.87**	**8**	0.13	0.14	<1	*Equus ferus*
34414.2	70	-9.65	-4.64	8							
	83	-7.05	-5.40	9	**-8.35**	**-5.02**	**8**	1.84	0.53	<1	*Equus ferus*
34414.4	91	-8.92	-4.30	8							
	77	-8.85	-4.33	7	**-8.89**	**-4.32**	**7**	0.05	0.02	<1	*Equus ferus*
34414.5	80	-9.49	-3.66	7							
	93	-9.41	-3.58	7	**-9.45**	**-3.62**	**7**	0.05	0.05	<1	*Equus ferus*
34415	76	-9.67	-3.59	7							
	100	-9.71	-3.95	6	**-9.69**	**-3.77**	**6**	0.02	0.25	<1	*Equus ferus*
34416	90	-11.05	-4.92	6							
	88	-11.02	-4.98	6	**-11.03**	**-4.95**	**6**	0.02	0.04	<1	*Equus ferus*
34417	86	-10.66	-7.35	6							
	79	-10.61	-7.20	7	**-10.64**	**-7.28**	**7**	0.03	0.10	<1	*Cervus elaphus*
34418	78	-9.75	-5.20	6							
	81	-10.02	-5.25	7	**-9.88**	**-5.23**	**6**	0.19	0.04	<1	*Equus hydrontinus*
34419	76	-10.43	-4.50	7							
	72	-10.30	-4.33	7	**-10.36**	**-4.42**	**7**	0.09	0.12	<1	*Equus ferus*
34420	89	-9.98	-3.12	8							
	86	-10.16	-2.94	7	**-10.07**	**-3.03**	**7**	0.13	0.13	<1	*Canis lupus*
34421	82	-9.69	-3.56	8							
	91	-9.69	-4.19	9	**-9.69**	**-3.87**	**8**	0.01	0.45	<1	*Vulpes* sp.
35034 (2)	72	-9.81	-4.59	12	**-9.81**	**-4.59**	**12**				*Oryctolagus cuniculus*
35036	76	-10.17	-6.28	11							
	74	-10.55	-6.50	12	**-10.36**	**-6.39**	**11**	0.27	0.16	<1	*Oryctolagus cuniculus*
35037	71	-9.15	-4.07	12							
	99	-9.84	-4.09	7	**-9.49**	**-4.08**	**9**	0.49	0.01	4	*Oryctolagus cuniculus*
35038	83	-9.25	-1.95	8							
	78	-9.08	-1.99	8	**-9.17**	**-1.97**	**8**	0.12	0.03	<1	*Oryctolagus cuniculus*
35045	79	-10.05	-4.63	6							
	71	-10.08	-4.74	6	**-10.06**	**-4.69**	**6**	0.02	0.08	<1	*Cervid*
35049	81	-8.83	-4.66	12	**-8.83**	**-4.66**	**12**				*Oryctolagus cuniculus*
35050	106	-10.77	-5.53	7							
	50	-10.78	-5.40	8	**-10.77**	**-5.47**	**7**	0.01	0.10	<1	*Oryctolagus cuniculus*
35051	67	-10.69	-5.85	9							
	93	-10.79	-5.94	8	**-10.74**	**-5.89**	**8**	0.07	0.06	<1	*Oryctolagus cuniculus*
35052	69	-12.78	-5.68	2							
	52	-12.61	-5.08	6	**-12.69**	**-5.38**	**4**	0.12	0.43	2	*Ursus* sp.
35053	69	-9.93	1.80	6							
	73	-10.21	1.47	5	**-10.07**	**1.64**	**5**	0.19	0.23	<1	*Capra pyreneica*
35054	88	-9.64	-2.53	7							
	103	-9.45	-3.07	9	**-9.55**	**-2.80**	**8**	0.14	0.38	1	*Capra pyreneica*
35056	50	-9.86	-2.92	7							
	96	-9.90	-3.26	7	**-9.88**	**-3.09**	**7**	0.03	0.24	<1	*Vulpes* sp.
35057	60	-9.35	-6.15	13							
	68	-9.51	-6.32	14	**-9.43**	**-6.23**	**13**	0.11	0.12	<1	*Equus hydrontinus*
35058	109	-10.75	-3.59	7							
	64	-11.26	-3.46	4	**-11.01**	**-3.53**	**5**	0.36	0.09	2	*Lynx spelaea*
35059	86	-11.85	-4.41	6							
	95	-11.95	-4.54	5	**-11.90**	**-4.48**	**5**	0.07	0.09	<1	*Crocuta sp.*
35060	89	-10.75	-4.74	7							
	71	-10.76	-4.81	7	**-10.76**	**-4.77**	**7**	0.01	0.05	<1	*Crocuta* sp.
35061	100	-14.14	-5.92	6							
	89	-14.12	-5.78	7	**-14.13**	**-5.85**	**6**	0.02	0.10	<1	*Crocuta* sp.
35062	91	-9.75	-2.37	6							
	53	-9.73	-2.41	5	**-9.74**	**-2.39**	**5**	0.02	0.03	<1	*Rupicapra rupicapra*
35063	56	-9.66	-3.53	7	**-9.66**	**-3.53**	**7**				*Rupicapra rupicapra*
35064	84	-10.52	-4.50	6							
	75	-10.50	-4.64	7	**-10.51**	**-4.57**	**7**	0.02	0.10	<1	*Cervus elaphus*
35065	71	-11.10	-3.77	6							
	75	-11.25	-3.78	3	**-11.17**	**-3.77**	**5**	0.11	0.01	2	*Cervus elaphus*
35066	75	-10.56	-2.40	5							
	97	-10.50	-2.39	3	**-10.53**	**-2.39**	**4**	0.05	0.00	2	*Canis* sp.
35067	85	-10.04	-7.41	7							
	86	-9.97	-7.51	6	**-10.01**	**-7.46**	**6**	0.05	0.07	<1	*Crocuta* sp.
35068	75	-8.61	-3.69	6							
	92	-8.66	-3.79	6	**-8.63**	**-3.74**	**6**	0.04	0.07	<1	*Rupicapra rupicapra*
34422	35	-12.03	-5.01	8	**-12.03**	**-5.01**	**8**				*Homo neanderthalensis*
34409	150	-9.39	-2.56	6	**-9.39**	**-2.56**	**6**				*Canis lupus*
34408 dirty enamel	62	-10.19	-5.03	12	**-10.19**	**-5.03**	**12**				*Canis lupus*
34408 clean enamel	170	-10.72	-2.75	5	**-10.72**	**-2.75**	**5**				*Canis lupus*

Table S19. Carbon and Oxygen isotope results for the Gabasa samples. Samples in red have been excluded because of their carbonate content >10%. Sample ID are "SEVA" numbers from the MPI-EVA.

- There was no statistically significant correlation between the layers where the samples were found and the $\delta^{13}C_{enamel}$ and $\delta^{18}O_{enamel}$ values of the Gabasa mammals (All samples: Kruskal-Wallis, chi-squared = 6.3293, df = 3, *p*-value =0.09664 and chi-squared = 1.84, df = 3, *p*-value = 0.6063, respectively; Non diagenetic samples: Kruskal-Wallis, chi-squared = 5.1531, df = 3, *p*-value =0.1609 and chi-squared = 2.7955, df = 3, *p*-value = 0.4242, respectively).
- $\delta^{13}C_{enamel}$ of the Gabasa mammals does not correlate to taxa (Kruskal-Wallis chi-squared = 22.302, df = 14, p-value = 0.1001) but a relationship seems to exist for $\delta^{18}O_{enamel}$ values (Kruskal-Wallis chi-squared = 26.603, df = 14, *p*-value = 0.032). Oxygen isotopes correlate with water dependency, and different taxa can have different drinking behaviors. This correlation is therefore not surprising.
- There was no influence between the associated environment of Gabasa mammal species and their $\delta^{13}C$ values (Kruskal-Wallis, chi-squared = 5.00, df = 2, *p*-value = 0.082), but a relationship seems to exist with $\delta^{18}O$ values (Kruskal-Wallis chi-squared = 10.607, df = 2, *p*-value = 0.004975). This relationship is however biased by the fact that the type of environments (mountain, open environment, forests) associated to the different mammal species was defined based on the species (i.e. the Iberian ibex and chamois are nowadays living in the mountains, therefore the mountain environment was attributed to them.
- There is no influence of tooth type sampled on the $\delta^{13}C$ and $\delta^{18}O$ values when carnivores and herbivores are considered together. Since carnivores (except bears and hyenas) are weaned early (56), we grouped the teeth into five groups, depending on the possibility of the animal being weaned during the formation time of the tooth sampled (in utero, weaned, not weaned, possibly weaned, unknown- unknown category was then excluded). In this case, the Kruskal-Wallis test is significant for the $\delta^{18}O$ values (Kruskal-Wallis chi-squared = 9.3796, df = 3, p-value = 0.02465). Teeth formed in utero and during the breastfeeding period showed higher ratios, consistent with the expected trend (Figure S10, S11, S12).

Here we notice that the mountain animals (*Rupicapra* sp. and *Capra pyrenaica*) are associated to the higher $\delta^{18}O_{enamel}$ values. This can be surprising since higher altitudes are usually associated with depleted $\delta^{18}O$ ("rainout effect") (57). Three of the six teeth analyzed for this "mountain" group were possibly formed during the breastfeeding period (M2) which could explain the abnormal $\delta^{18}O$ of the chamois, except that their values overlap with those of the teeth formed after the weaning with only one exception (an exceptionally high $\delta^{18}O_{enamel}$ value of 1.6 ‰, Figure S10). As the fractionation between the isotope composition of the drinking water ($\delta^{18}O_W$) and the isotope composition of the oxygen

integrated into the carbonate fraction of the enamel ($\delta^{18}O_{enamel}$) is species dependent, the observed variations between species could be related to their specific metabolism. We therefore converted the $\delta^{18}O_{carbonate}$ into $\delta^{18}O_{phosphate}$ using the equations of Iacumin et al. (1996) and then used all the equations specific to each species allowing to convert the $\delta^{18}O_{phosphate}$ into the $\delta^{18}O$ of the drinking water (58–63). The aim was to see if there would be a homogenization of the $\delta^{18}O$ values between species, but the trends were actually similar to the non-corrected data. In Payre, the more elevated $\delta^{18}O_{enamel}$ values observed in chamois have been explained by drinking water at a higher altitude (only 100 m) originating from rainfalls, whereas drinking water from the Rhone River in the valley comes from the Alps (i.e., fed by ^{18}O-depleted meltwater). In addition, evaporation on limestone plateaus enhanced the enrichment in ^{18}O. The Los Moros cave of Gabasa is located close to the source of a small river, Rio Sosa, at 780 m altitude (Figure 1) (64). At higher altitudes (between 800 and 1100 m, Figure 1), the drinking water probably also originates from rainfall, with possible evaporation, which might explain the higher range observed in ibex and chamois. The animals living in the valley could also drink from the Sosa River.

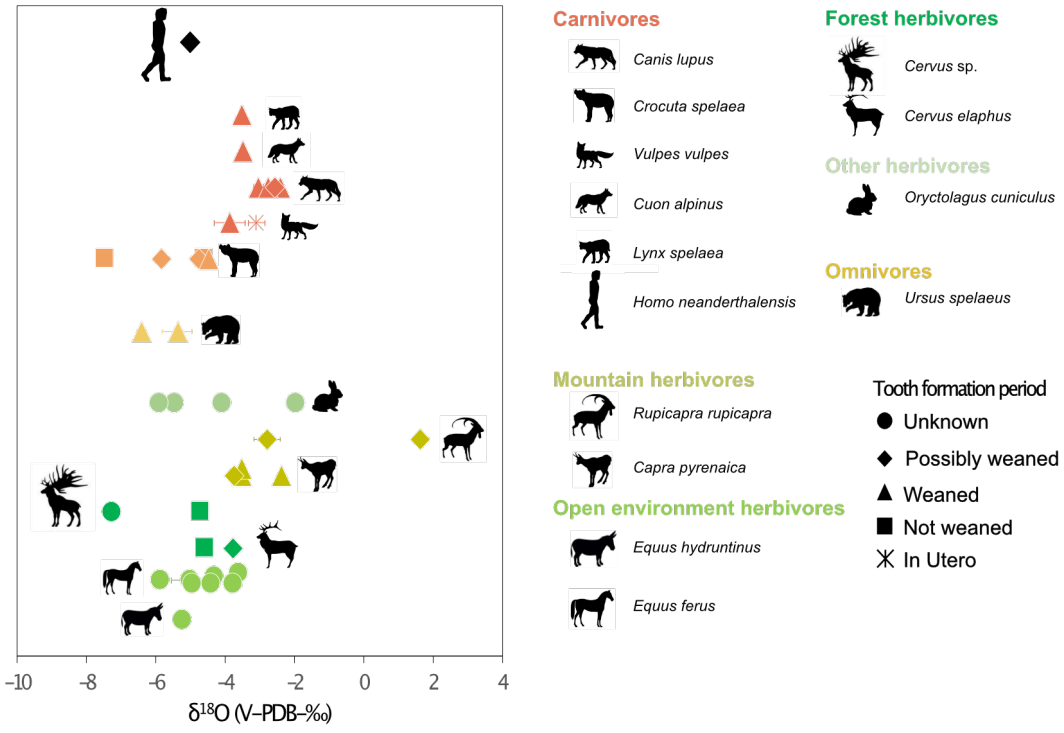

Figure S10. Oxygen isotope ratios in dental enamel of Gabasa mammals.

Among the carnivores, $\delta^{18}O_{enamel}$ values are positively correlated with $\delta^{13}C_{enamel}$ (Figure S12). The lowest values are associated with cave animals (hyenas and cave bears) and the highest with wolves and foxes. The observed trends are similar to those described in the Payre site, France, where cave bears showed

low $\delta^{13}C_{enamel}$ and $\delta^{18}O_{enamel}$ values and chamois elevated ones (65, 66). The Neandertal also exhibited intermediate $\delta^{18}C_{enamel}$ and $\delta^{18}O_{enamel}$ values, between those of cave animals and wolves (66).

More elevated $\delta^{13}C_{enamel}$ in horses and chamois compared to forest animals' values (red deer) can be explained by the consumption of vegetation growing in more arid regions (open environment and mountain) (67).

Considering the possible $\delta^{13}C_{enamel}$ offset of about 1.3 ‰ between carnivores and herbivores (68), wolves and foxes likely fed on mountain herbivores and did not hunt in the closed forest environments. The large differences in $\delta^{13}C_{enamel}$ values between different hyena individuals show this predator is more opportunistic. The low $\delta^{13}C_{enamel}$ of cave bears have been hypothesized as the result of herbivory and not hibernation (69). The herbivores showing the closest $\delta^{13}C_{enamel}$ and $\delta^{18}O_{enamel}$ to Neandertals are rabbits, horses and deer (Figure S12).

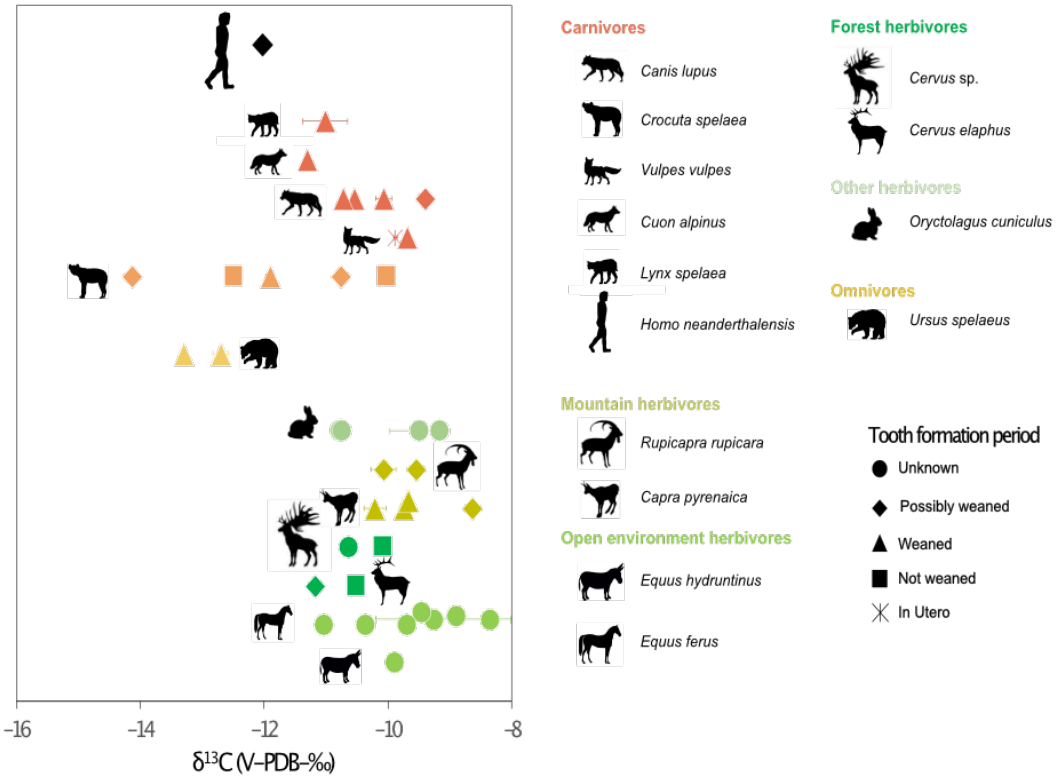

Figure S11. Carbon isotope ratios in dental enamel of Gabasa mammals.

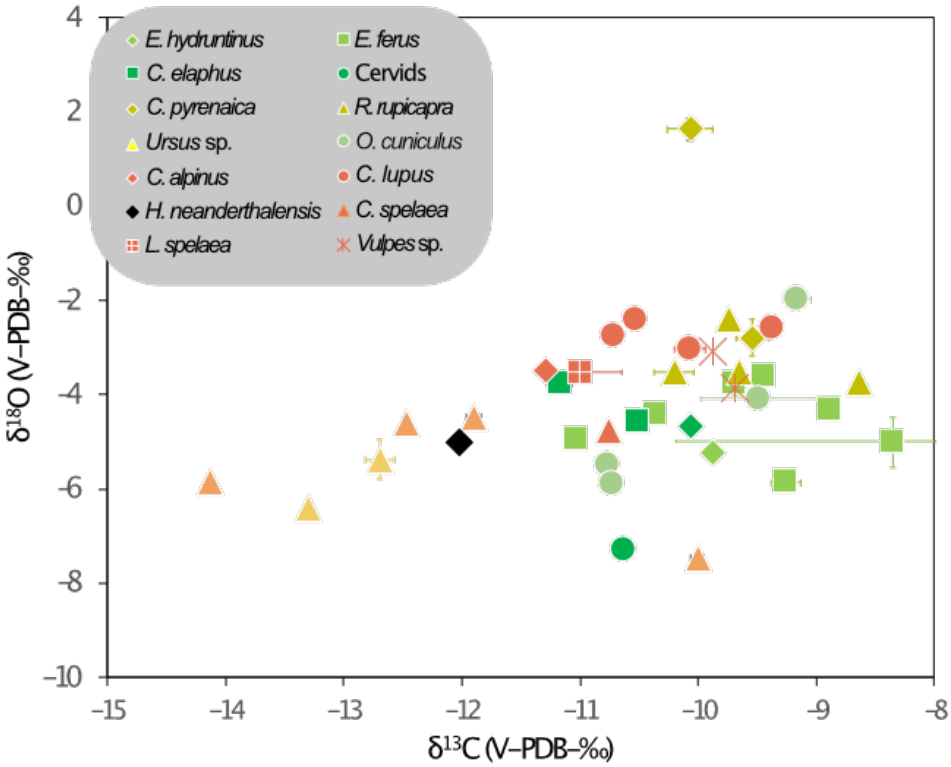

Figure S12. O and C isotope ratios in dental enamel of Gabasa mammals grouped by species.

Supplementary Information 7

Supplementary information on trace element results and discussion

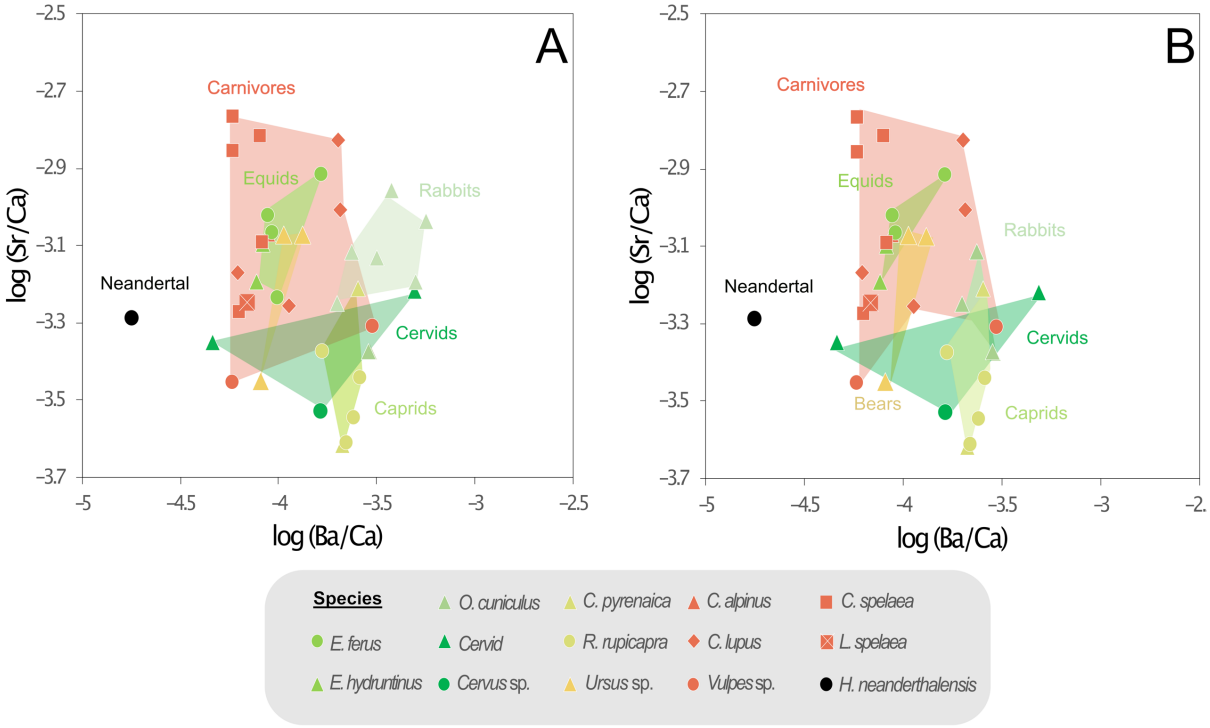

Figure S13. Ba/Ca and Sr/Ca ratios A. in the different teeth of Gabasa grouped by species B. in different teeth of Gabasa mammals, without teeth showing evidences of soil contamination, grouped by diet.

In a 2005 study, Sponheimer and collaborators (70) demonstrated that grazers tend to have higher Sr/Ca and Ba/Ca ratios compared to carnivores and browsers. Accordingly, we observe higher Sr/Ca ratios in grazers (Equids) compared to browsers and mixed feeders (Cervids and Caprids) but overlap with the carnivores and the bears. The Neandertal individual had the lowest Ba/Ca ratio of our assemblage but not the lowest Sr/Ca (Table S18). For all enamel data, there is no correlation between Ba/Ca and Sr/Ca, unlike previously observed data in teeth (71). This can likely be explained by the heterogeneous nature of the analyzed teeth (i.e., belonging to different stages of development, different species, and coming from animals from diverse ecology).

Diet	Ba/Ca	Sr/Ca
In Utero	Low	Low
Exclusive breastfeeding	Increasing	Lowest
Introduction of solid food	Still high	Increasing (especially with plants)
Post weaning	Decreasing	High if plant consumption

Table S20. Summary of Sr/Ca and Ba/Ca trends observed in dental enamel depending on the diet of a mammal (source Tsutaya and Yoneda, 2015) (72)

Additional figures

Figure S14 Comparison of Zn isotope ratios analyzed in different terrestrial food webs (28–30, 35, 73)

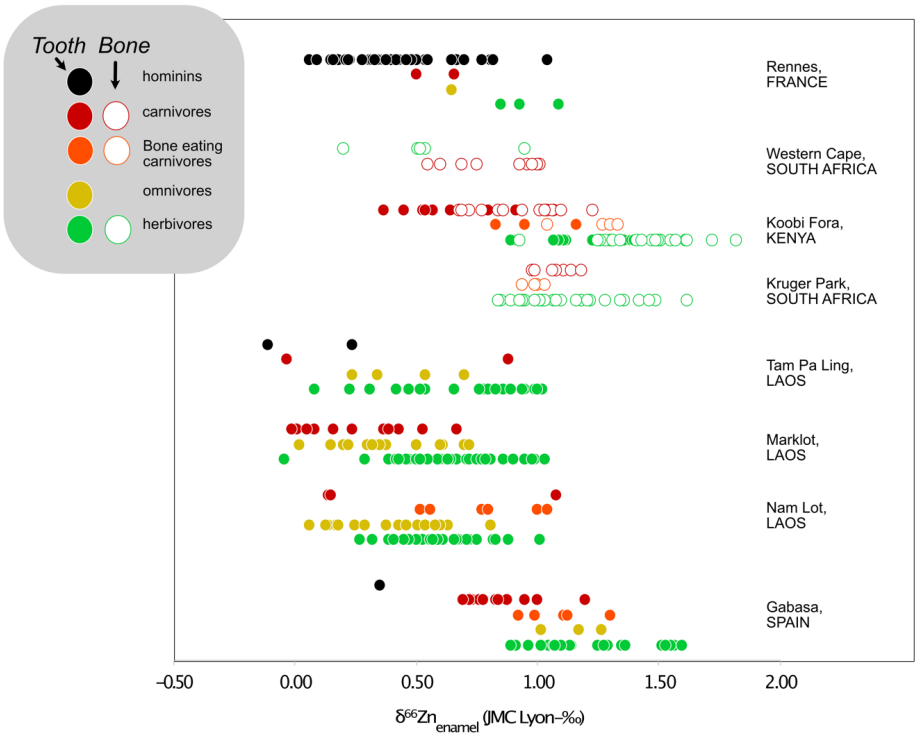

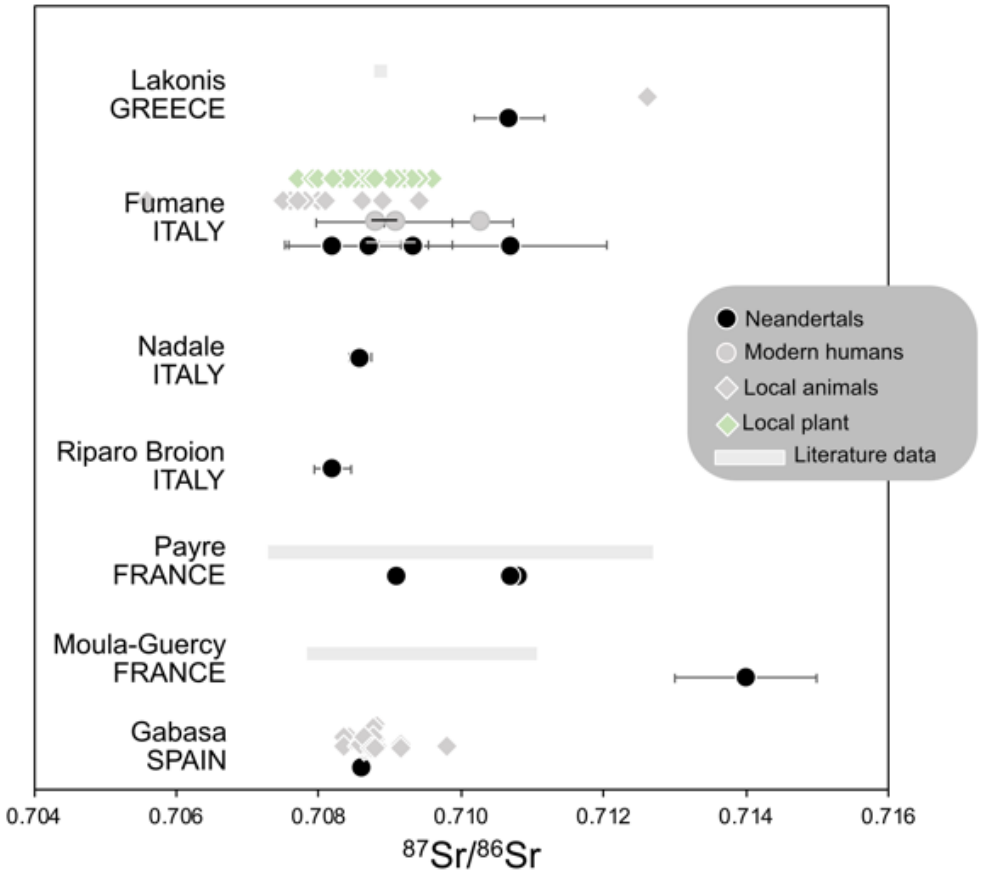

Figure S15 Comparison of Sr isotope ratios analyzed in different teeth of Neandertals found in Europe (74–79)**.** Gabasa's data are from this study.

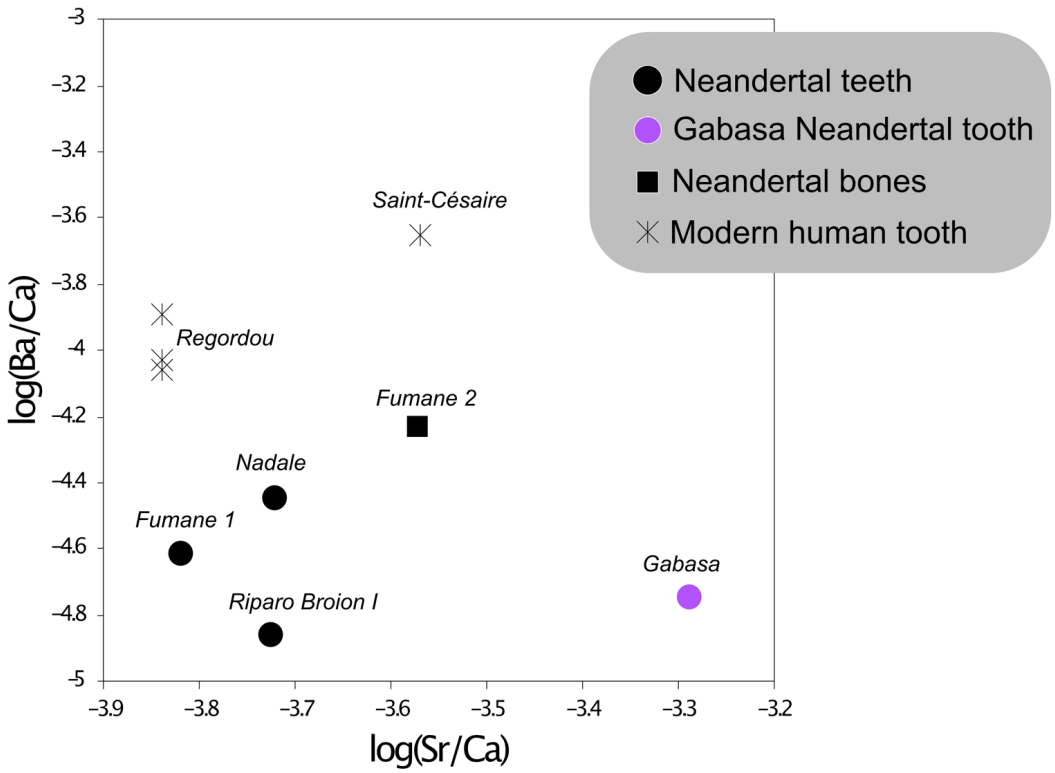

Figure S16 Strontium and Barium to Calcium ratios in Neanderthals bones and teeth (76, 80, 81) Gabasa's data are from this study.

-

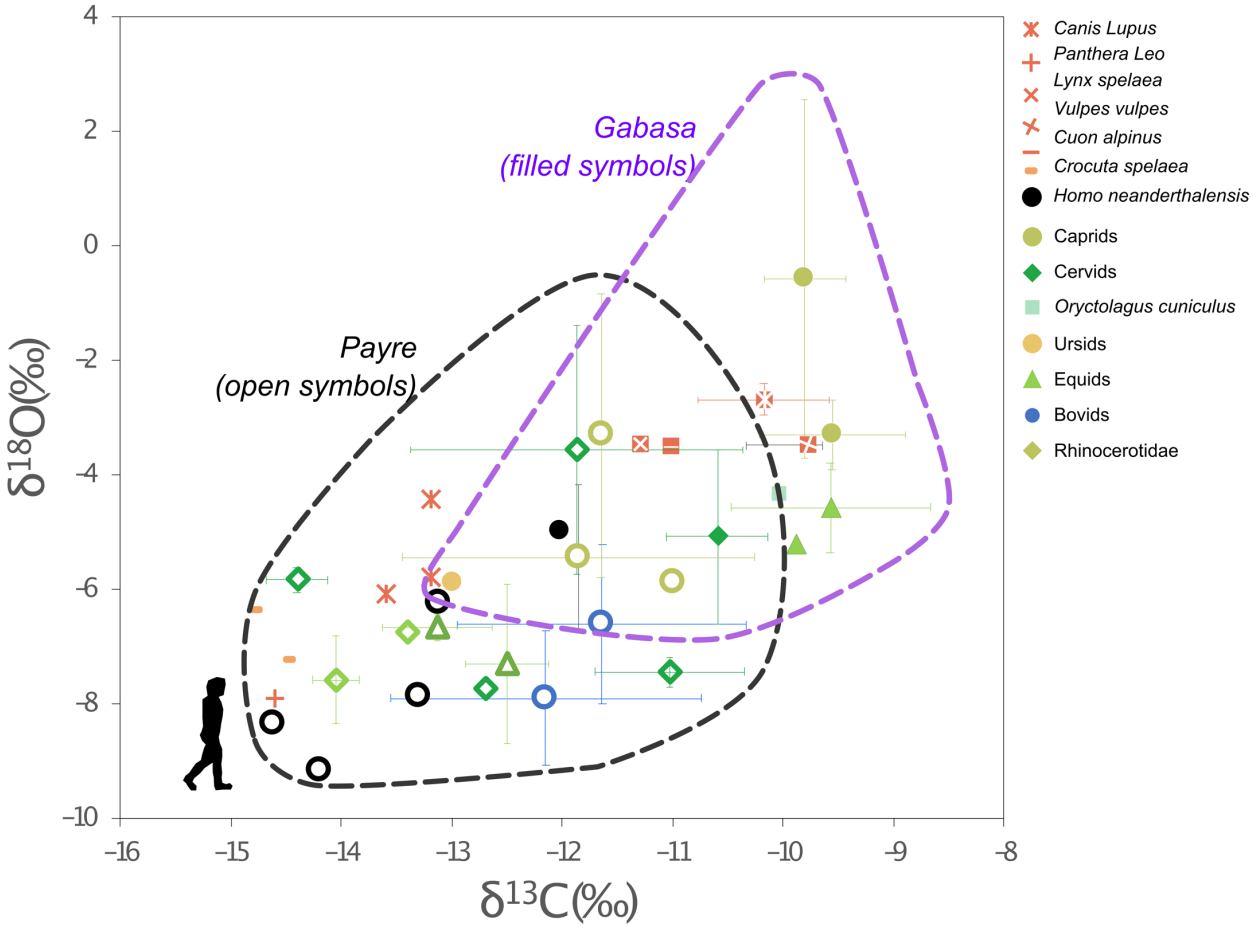

Figure S17 Carbon and oxygen isotope data in dental enamel of Neandertals and associated fauna from Western European sites. (65, 66) Gabasa data are from this study.

References

1. F. Moynier, D. Vance, T. Fujii, P. Savage, The isotope geochemistry of zinc and copper. Reviews in Mineralogy and Geochemistry **82**, 543–600 (2017).

2. S. Pichat, C. Douchet, F. Albarède, Zinc isotope variations in deep-sea carbonates from the eastern equatorial Pacific over the last 175 ka. Earth and Planetary Science Letters **210**, 167–178 (2003).

3. C. Boix, et al., Larger foraminifera distribution and strontium isotope stratigraphy of the La Cova limestones (Coniacian–Santonian,"Serra del Montsec", Pyrenees, NE Spain). Cretaceous Research **32**, 806–822 (2011).

4. V. Villalba-Mouco, et al., Territorial mobility and subsistence strategies during the Ebro Basin Late Neolithic-Chalcolithic: A multi-isotope approach from San Juan cave (Loarre, Spain). Quaternary International **481**, 28–41 (2018).

5. E. Caus, G. Frijia, M. Parente, R. Robles-Salcedo, R. Villalonga, Constraining the age

of the last marine sediments in the late Cretaceous of central south Pyrenees (NE Spain): Insights from larger benthic foraminifera and strontium isotope stratigraphy. Cretaceous Research **57**, 402–413 (2016).

6. J. Hoogewerff, Data for: Bioavailable $^{87}Sr/^{86}Sr$ in European soils: a baseline for provenancing studies. Science of the Total Environment **672** 1033-1044 (2019).

7. I. Sarasketa-Gartzia, V. Villalba-Mouco, P. Le Roux, Á. Arrizabalaga, D. C. Salazar-García, Anthropic resource exploitation and use of the territory at the onset of social complexity in the Neolithic-Chalcolithic Western Pyrenees: a multi-isotope approach. Archaeological and Anthropological Sciences **11**, 3665–3680 (2019).

8. A. Sopeña, Y. Sánchez-Moya, E. Barrón, New palynological and isotopic data for the Triassic of the western Cantabrian Mountains (Spain). Journal of Iberian Geology, **35 (1)** 35-45 (2010).

9. A. Travé, P. Labaume, F. Calvet, A. Soler, Sediment dewatering and pore fluid migration along thrust faults in a foreland basin inferred from isotopic and elemental geochemical analyses (Eocene southern Pyrenees, Spain). Tectonophysics **282**, 375–398 (1997).

10. A. Lopez-Galindo, A. B. Aboud, P. F. Hach-Ali, J. C. Ruiz, Mineralogical and geochemical characterization of palygorskite from Gabasa (NE Spain). Evidence of a detrital precursor. Clay Minerals **31**, 33–44 (1996).

11. MapasIGME - Spanish Geological Survey maps: Geological map 200k. Synthesis of existing maps - Sheet number 23 (HUESCA) (April 10, 2020).

12. L. Montes, P. Utrilla, The cave of Los Moros-1 at Gabasa (Huesca). in *Pleistocene and Holocene Hunters-Gatherers in Iberia and the Gibraltar Strait. The Current Archaeological Record*. Ed: Robert Sala Ramos. Universidad de Burgos-Fundación Atapuerca, 181–188 (2014).

13. M. Hoyos, P. Utrilla, L. Montes, J. A. Cuchi, Estratigrafía, sedimentología y paleoclimatología de los depósitos musterienses de la Cueva de los Moros de Gabasa. Cuaternario y geomorfología **6**, 143–155 (1992).

14. M. F. Blasco, In the pursuit of game: The Mousterian cave site of Gabasa 1 in the Spanish Pyrenees. Journal of Anthropological Research **53**, 177–217 (1997).

15. F. Blasco Sancho, Hombres, fieras y presas: estudio arqueozoológico y tafonómico del yacimiento del Paleolítico Medio de la Cueva de Gabasa 1 (Huesca) (Universidad de Zaragoza, Spain, 1995).

16. P. Utrilla, L. Montes, F. Blasco, T. Torres, J. E. Ortiz, La cueva de Gabasa revisada 15 años después: un cubil para las hienas y un cazadero para los Neandertales. Zona Arqueológica **13**, 376–389 (2010).

17. L. Montes, P. Utrilla, R. Hedges, Le passage Paléolithique Moyen-Paléolithique Supérieur dans la Vallée de l'Ebre (Espagne). Datations radiométriques des grottes de Peña Miel et Gabasa. Trabalhos de Arqueologia **17,** 87-102 (2001)

18. P. González-Sampériz, L. Montes, P. Utrilla, Pollen in hyena coprolites from Gabasa Cave (northern Spain). Review of Palaeobotany and Palynology **126**, 7–15 (2003).

19. A. Boscaini, J. Madurell-Malapeira, M. Llenas, B. Martínez-Navarro, The origin of the critically endangered Iberian lynx: Speciation, diet and adaptive changes. Quaternary Science Reviews **123**, 247–253 (2015).

20. J. C. Reynolds, N. J. Aebischer, Comparison and quantification of carnivore diet by faecal analysis: a critique, with recommendations, based on a study of the fox Vulpes vulpes. Mammal Review **21**, 97–122 (1991).

21. C. Bon, et al., Coprolites as a source of information on the genome and diet of the cave hyena. Proceedings of the Royal Society B: Biological Sciences **279**, 2825–2830 (2012).

22. C. G. Diedrich, K. Zák, Prey deposits and den sites of the Upper Pleistocene hyena Crocuta crocuta spelaea (Goldfuss, 1823) in horizontal and vertical caves of the Bohemian Karst (Czech Republic). Bulletin of Geosciences **81**, 237–276 (2006).

23. T. M. Newsome, et al., Food habits of the world's grey wolves. Mammal Review **46**, 255–269 (2016).

24. J. Lanszki, M. Márkus, D. Újváry, Á. Szabó, L. Szemethy, Diet of wolves Canis lupus returning to Hungary. Acta theriologica **57**, 189–193 (2012).

25. C. Capitani, I. Bertelli, P. Varuzza, M. Scandura, M. Apollonio, A comparative analysis of wolf (Canis lupus) diet in three different Italian ecosystems. Mammalian biology **69**, 1–10 (2004).

26. J.-B. Mallye, et al., Caractérisation des coprocénoses produites par le loup et le dhole et transfert au fossile in *Relations Hommes/Canidés de La Préhistoire Aux Périodes Modernes* (2018).

27. J. F. Kamler, A. Johnson, C. Vongkhamheng, A. Bousa, The diet, prey selection, and activity of dholes (*Cuon alpinus*) in northern Laos. Journal of Mammalogy **93**, 627–633 (2012).

28. K. Jaouen, M. Beasley, M. Schoeninger, J.-J. Hublin, M. P. Richards, Zinc isotope ratios of bones and teeth as new dietary indicators: results from a modern food web (Koobi Fora, Kenya). Scientific Reports **6**, 26281 (2016).

29. N. Bourgon, et al., Zinc isotopes in Late Pleistocene fossil teeth from a Southeast Asian cave setting preserve paleodietary information. Proceedings of the National Academy of Sciences **117**, 4675–4681 (2020).

30. N. Bourgon, et al., Trophic ecology of a Late Pleistocene early modern human from tropical Southeast Asia inferred from zinc isotopes. Journal of Human Evolution **161**, 103075 (2021).

31. J. McCormack, et al., Trophic position of Otodus megalodon and great white sharks through time revealed by zinc isotopes. Nature Communications (2022) **13 (1)** 2980 https://doi.org/10.1038/s41467-022-30528-9

32. K. Jaouen, P. Szpak, M. P. Richards, Zinc isotope ratios as indicators of diet and trophic level in arctic marine mammals. PLOS One **11**, e0152299 (2016).

33. K. Jaouen, et al., Zinc isotope variations in archeological human teeth (Lapa do Santo, Brazil) reveal dietary transitions in childhood and no contamination from gloves. PLOS One **15**, e0232379 (2020).

34. K. Jaouen, Les isotopes stables des métaux de transition (Cu, Fe, Zn) au service de l'anthropologie. Ecole Normale Supérieure de Lyon et Université Lyon **1** (2012).

35. K. Jaouen, et al., Tracing intensive fish and meat consumption using Zn isotope ratios: evidence from a historical Breton population (Rennes, France). Scientific Reports **8**, 1–12 (2018).

36. H. B. Vonhof, et al., High-precision stable isotope analysis of <5 μg $CaCO_3$ samples by continuous-flow mass spectrometry. Rapid Communications in Mass Spectrometry **34**, e8878 (2020).

37. W. Stichler, Interlaboratory comparison of new materials for carbon and oxygen isotope ratio measurements in *Reference and Intercomparison Materials for Stable Isotopes of Light Elements*, (Citeseer, 1995), pp. 67–74.

38. , GeoReM - Query by reference samples or materials (published values) (January 17, 2022).

39. D. Yeghicheyan, et al., A New Interlaboratory Characterisation of Silicon, Rare Earth Elements and Twenty-Two Other Trace Element Concentrations in the Natural River Water Certified Reference Material SLRS-6 (NRC-CNRC). Geostandards and Geoanalytical Research **43**, 475–496 (2019).

40. P. L. Koch, N. Tuross, M. L. Fogel, The Effects of Sample Treatment and Diagenesis on the Isotopic Integrity of Carbonate in Biogenic Hydroxylapatite. Journal of Archaeological Science **24**, 417–429 (1997).

41. Y. Wang, T. E. Cerling, A model of fossil tooth and bone diagenesis: implications for paleodiet reconstruction from stable isotopes. Palaeogeography, Palaeoclimatology, Palaeoecology **107**, 281–289 (1994).

42. B. Reynard, V. Balter, Trace elements and their isotopes in bones and teeth: Diet, environments, diagenesis, and dating of archeological and paleontological samples. Palaeogeography, Palaeoclimatology, Palaeoecology **416**, 4–16 (2014).

43. K. Jaouen, What is our toolbox of analytical chemistry for exploring ancient hominin diets in the absence of organic preservation? Quaternary Science Reviews **197**, 307–318 (2018).

44. M. J. Kohn, J. Morris, P. Olin, Trace element concentrations in teeth – a modern Idaho baseline with implications for archeometry, forensics, and palaeontology. Journal of Archaeological Science **40**, 1689–1699 (2013).

45. T. Tacail, et al., Assessing human weaning practices with calcium isotopes in tooth enamel. Proceedings of the National Academy of Sciences **114**, 6268–6273 (2017).

46. C. J. Brown, et al., Environmental influences on the trace element content of teeth—implications for disease and nutritional status. Archives of Oral Biology **49**, 705–717 (2004).

47. F. O. Falla-Sotelo, et al., Analysis and discussion of trace elements in teeth of different animal species. Braz. J. Phys. **35**, 761–762 (2005).

48. K. Grünke, H.-J. Stärk, R. Wennrich, U. Franck, Determination of traces of heavy metals (Mn, Cu, Zn, Cd and Pb) in microsamples of teeth material by ETV-ICP-MS. Fresenius' journal of analytical chemistry **354**, 633–635 (1996).

49. M. E. Fleet, Carbonated Hydroxyapatite: Materials, Synthesis, and Applications (CRC Press, 2014).

50. S. R. Copeland, et al., Strontium isotope ratios ($^{87}Sr/^{86}Sr$) of tooth enamel: a comparison of solution and laser ablation multicollector inductively coupled plasma mass spectrometry methods. Rapid Communications in Mass Spectrometry: An International Journal Devoted to the Rapid Dissemination of Up-to-the-Minute Research in Mass Spectrometry **22**, 3187–3194 (2008).

51. W. Müller, et al., Enamel mineralization and compositional time-resolution in human teeth evaluated via histologically-defined LA-ICPMS profiles. Geochimica et Cosmochimica Acta **255**, 105–126 (2019).

52. S. Safont, A. Malgosa, M. E. Subirà, J. Gibert, Can trace elements in fossils provide information about palaeodiet? International Journal of Osteoarchaeology **8**, 23–37 (1998).

53. S. S. Hakki, et al., Dietary boron does not affect tooth strength, micro-hardness, and density, but affects tooth mineral composition and alveolar bone mineral density in rabbits fed a high-energy diet. Journal of Trace Elements in Medicine and Biology **29**, 208–215 (2015).

54. A. Rodríguez-Hidalgo, et al., Feeding behaviour and taphonomic characterization of non-ingested rabbit remains produced by the Iberian lynx (*Lynx pardinus*). Journal of Archaeological Science **40**, 3031–3045 (2013).

55. R. Villalonga, et al., Larger foraminifera and strontium isotope stratigraphy of middle Campanian shallow-water lagoonal facies of the Pyrenean Basin (NE Spain). Facies **65**, 1–23 (2019).

56. H. E. Watts, J. B. Tanner, B. L. Lundrigan, K. E. Holekamp, Post-weaning maternal effects and the evolution of female dominance in the spotted hyena. Proceedings of the Royal Society B: Biological Sciences **276**, 2291–2298 (2009).

57. P. K. Swart, K. C. Lohmann, J. McKenzie, S. Savin, Climate change in continental isotopic records. Washington DC American Geophysical Union Geophysical Monograph Series **78** (1993).

58. P. Iacumin, A. Longinelli, Relationship between $\delta^{18}O$ values for skeletal apatite from reindeer and foxes and yearly mean $\delta^{18}O$ values of environmental water. Earth and Planetary Science Letters **201**, 213–219 (2002).

59. D. d'Angela, A. Longinelli, Oxygen isotopes in living mammal's bone phosphate: further results. Chemical Geology: Isotope Geoscience section **86**, 75–82 (1990).

60. P. Iacumin, H. Bocherens, A. Mariotti, A. Longinelli, Oxygen isotope analyses of co-existing carbonate and phosphate in biogenic apatite: a way to monitor diagenetic alteration of bone phosphate? Earth and Planetary Science Letters **142**, 1–6 (1996).

61. A. D. Huertas, P. Iacumin, B. Stenni, B. S. Chillón, A. Longinelli, Oxygen isotope variations of phosphate in mammalian bone and tooth enamel. Geochimica et Cosmochimica Acta **59**, 4299–4305 (1995).

62. J. D. Bryant, P. L. Koch, P. N. Froelich, W. J. Showers, B. J. Genna, Oxygen isotope partitioning between phosphate and carbonate in mammalian apatite. Geochimica et Cosmochimica Acta **60**, 5145–5148 (1996).

63. M. Kohn, T. Cerling, Stable Isotope Compositions of Biological Apatite. Reviews in Mineralogy and Geochemistry **48** (2002).

64. J. I. Lizalde, P. Utrilla, L. Montes, Les neandertales de la Grotte de los Moros de Gabasa (Huesca). in *Colloque de la Commision VIII de l' UISPP*. Vila Nova de Foz Côa (1999).

65. H. Bocherens, et al., Direct isotopic evidence for subsistence variability in Middle Pleistocene Neanderthals (Payre, southeastern France). Quaternary Science Reviews **154**, 226–236 (2016).

66. M. Ecker, et al., Middle Pleistocene ecology and Neanderthal subsistence: insights from stable isotope analyses in Payre (Ardeche, southeastern France). Journal of Human Evolution **65**, 363–373 (2013).

67. R. E. Stevens, R. E. M. Hedges, Carbon and nitrogen stable isotope analysis of northwest European horse bone and tooth collagen, 40,000BP–present: Palaeoclimatic interpretations. Quaternary Science Reviews **23**, 977–991 (2004).

68. H. Bocherens, D. Drucker, Trophic level isotopic enrichment of carbon and nitrogen in bone collagen: case studies from recent and ancient terrestrial ecosystems. International Journal of Osteoarchaeology **13**, 46–53 (2003).

69. E. Trinkaus, M. P. Richards, Reply to Grandal and Fernández: Hibernation can also cause high $\delta^{15}N$ values in cave bears. Proceedings of the National Academy of Sciences **105**, E15–E15 (2008).

70. M. Sponheimer, D. de Ruiter, J. Lee-Thorp, A. Späth, Sr/Ca and early hominin diets revisited: new data from modern and fossil tooth enamel. Journal of Human Evolution **48**, 147–156 (2005).

71. Q. Li, et al., Spatially-resolved Ca isotopic and trace element variations in human deciduous teeth record diet and physiological change. Environmental Archaeology **Ahead of Print**, 1–10 (2020).

72. T. Tsutaya, M. Yoneda, Reconstruction of breastfeeding and weaning practices using stable isotope and trace element analyses: A review. American Journal of Physical

Anthropology **156**, 2–21 (2015).

73. K. Jaouen, M.-L. Pons, V. Balter, Iron, copper and zinc isotopic fractionation up mammal trophic chains. Earth and Planetary Science Letters **374**, 164–172 (2013).

74. M. Willmes, et al., A comprehensive chronology of the Neanderthal site Moula-Guercy, Ardèche, France. Journal of Archaeological Science: Reports **9**, 309–319 (2016).

75. M. P. Richards, et al., Strontium isotope evidence for Neanderthal and modern human mobility at the upper and middle palaeolithic site of Fumane Cave (Italy). PLOS One **16**, e0254848 (2021).

76. A. Nava, et al., Early life of Neanderthals. Proceedings of the National Academy of Sciences **117**, 28719–28726 (2020).

77. M. Richards, et al., Strontium isotope evidence of Neanderthal mobility at the site of Lakonis, Greece using laser-ablation PIMMS. Journal of Archaeological Science **35**, 1251–1256 (2008).

78. A. Benson, et al., Laser ablation depth profiling of U-series and Sr isotopes in human fossils. Journal of Archaeological Science **40**, 2991–3000 (2013).

79. M.-H. Moncel, P. Fernandes, M. Willmes, H. James, R. Grün, Rocks, teeth, and tools: New insights into early Neanderthal mobility strategies in South-Eastern France from lithic reconstructions and strontium isotope analysis. PLOS One **14**, e0214925 (2019).

80. P.-J. Dodat, et al., Isotopic calcium biogeochemistry of MIS 5 fossil vertebrate bones: application to the study of the dietary reconstruction of Regourdou 1 Neandertal fossil. Journal of Human Evolution **151**, 102925 (2021).

81. V. Balter, et al., Les Néandertaliens étaient-ils essentiellement carnivores? Résultats préliminaires sur les teneurs en Sr et en Ba de la paléobiocénose mammalienne de Saint-Césaire. Comptes Rendus de l'Académie des Sciences-Series IIA-Earth and Planetary Science **332**, 59–65 (2001).